# REPORT DOCUMENTATION PAGE

Form Approved
OMB No. 0704-0188



| 1. AGENCY USE ONLY (Leave blank) | 2. REPORT DATE | 3. REPORT TYPE AND DATES COVERED |
|---|---|---|
| | 31-December-2000 | Final Report: 4/25/00 - 12/31/00 |

**4. TITLE AND SUBTITLE**

Ink-Jet Printing of Gradient Index of Refraction Lenses

**5. FUNDING NUMBERS**

Contract #
DAAH01-00-C-R125

**6. AUTHOR(S)**

W. Royall Cox

**7. PERFORMING ORGANIZATION NAME(S) AND ADDRESS(ES)**

MicroFab Technologies, Inc.
1104 Summit Avenue, Suite 110
Plano, Texas 75074

**8. PERFORMING ORGANIZATION REPORT NUMBER**

RS01 - Final Report

**9. SPONSORING/MONITORING AGENCY NAME(S) AND ADDRESS(ES)**

Department of the Army
United States Army Aviation and Missile Command
Redstone Arsenal, Alabama 35898-5000

**10. SPONSORING/MONITORING AGENCY REPORT NUMBER**

**11. SUPPLEMENTARY NOTES**

The views, opinions and/or findings contained in this report are those of the author(s) and should not be construed as an official Department of the Army position, policy or decision, unless so designated by other documentation.

**12a. DISTRIBUTION/AVAILABILITY STATEMENT**

Approved for public release; distribution unlimited

**12b. DISTRIBUTION CODE**

**13. ABSTRACT** *(Maximum 200 words)*

This is the Phase I Final Report developed under SBIR contract for topic # SB001-010. The overall technical objective was to design a rapid-prototyping/manufacturing machine capable of fabricating GRIN (gradient index of refraction) lenses as large as 6 inches in diameter by direct-write, 3D inkjet printing processes, using CAD files of optical models as input data. The design of this GRIN Lens Printing Platform was completed, and a bill of materials was generated with vendors, model numbers and prices for all key systems, subsystems and components. In addition, a set of UV-curing optical epoxy "inks" of differing indexes of refractive was developed and used in test printing of small gradient index lenses, in order to study material interactions and to verify printing process concepts. Ongoing efforts to increase the temperature capability of our print heads is expected to enable the printing of low-melting IR (infrared) glasses, which would extend the application wavelengths of printed GRIN lenses from the near to the middle and far IR. Successful development of this machine during a Phase II effort would enable both greater flexibility in GRIN lens design & fabrication and significant cost reductions in the fabrication of a wide range of optical elements.

| 14. SUBJECT TERMS | 15. NUMBER OF PAGES |
|---|---|
| SBIR Report; GRIN lens fabrication; inkjet printing. | 35 |
| | 16. PRICE CODE |

| 17. SECURITY CLASSIFICATION OF REPORT | 18. SECURITY CLASSIFICATION OF THIS PAGE | 19. SECURITY CLASSIFICATION OF ABSTRACT | 20. LIMITATION OF ABSTRACT |
|---|---|---|---|
| UNCLASSIFIED | UNCLASSIFIED | UNCLASSIFIED | UL |

# Ink-Jet Printing of Gradient Index of Refraction Lenses

**December 29, 2000**

**Sponsored by**
**Defense Advanced Research Project Agency (DOD)**
**ARPA Order D611/85**

**Issued by**
**U.S. Army Aviation and Missile Command Under**
**Contract No. DAAH01-00-C-R125**

## Final Report

for

**April 25, 2000 - December 31, 2000**

by
W. Royall Cox, Ph.D.
Principal Scientist & Project Principal Investigator
with major contributions from:
Scott Ayers, Hahns-Jochen Trost, Michael Grove & Rick Hoenigman

MicroFab Technologies, Inc.
1104 Summit Ave., Suite 110
Plano, Texas 75074
Phone: (972)578-8076 / Fax: (972)423-2438 / Email: rcox@microfab.com

Contract Start Date: 27 April, 2000
Contract Expiration Date: 2 December, 2000

# 1.0 Summary

The overall objective of this SBIR Phase-I project has been to design a machine capable of fabricating GRIN (gradient index of refraction) optical lenses up to 6" in diameter by direct-write, 3D inkjet printing processes, which would enable both significant manufacturing cost reductions and superior optical performance of fabricated lenses relative to traditional mechanical machining of such components. This objective has been met during the Phase-I work period. As a rapid-prototyping/manufacturing tool, this printing platform will also be able to compete in cost with current methods for optics and micro-optics production and have will have additional, unique capabilities for in-situ integration in optical device manufacture, such as direct writing of microlenses on optical devices (e.g., diode lasers & detectors) and components (e.g., fibers, lenses & waveguides) The key technical challenges associated with optimization of machine functionality in GRIN macro-lens printing were identified and addressed, in part by performing experiments with the printing of GRIN mini/micro-lenses using an existing micro-optics printing station and an ink-jet-printable set of original optical polymer formulations having differing refractive indices.

The work during Phase-I was organized into four task areas: machine design; initial optical material system identification and testing; initial printing process development; and GRIN lens modeling. The milestone associated with each task area was achieved and the key results may be summarized as follows:

(1) GRIN Lens Printing Station Design:
The designs of the system and the key subsystems for a stand-alone GRIN Lens Printing Platform were completed, including a bill of materials with current pricing of individual components and the software approach required. Here four print heads containing optical formulations of differing index of refraction dispense droplets onto a rotating support substrate, in order to build up lenses in a layer-by-layer fashion from data input as CAD file cross-sections developed from optical models.

(2) Optical Materials System Development:
The optical material system determined to be best suited for fabrication of GRIN lenses by ink-jet printing is a rheologically compatible set of different mixtures of optical monomers and oligomers which are formulated to span a refractive index range of at least 0.15 and to be polymerized by UV (ultraviolet) irradiation after printing. After further development to increase the maximum operating temperature of MicroFab print heads, from 300°C (currently) to 500°C, the printing of low-melting IR (infrared) glasses would be readily accomplished by this machine.

(3) GRIN Lens Printing Process Development:
A microlens printing system having two print heads containing optical fluids of differing refractive index was used to print small GRIN lenses, in order to determine key process features which will be incorporated in the GRIN Lens Printing Platform to control such variables as inter-diffusion between adjacently deposited materials of differing index and uniformity of curing throughout relatively large volumes.

(4) GRIN Lens Design, Modeling and Performance Characterization:
Modeling of GRIN lenses of various configuration has shown quantitatively in impact of parameters such as refractive index spread and lens thickness on key optical performance factors such focal length, focal spot size and imaging quality. Optical characterization of small printed GRIN lenses has shown how the printing process may be varied to achieve specific performance features.

## 2.0 Phase-I Technical Results

The work performed and results obtained on each project milestone/objective is summarized below, with some of the details being left to the Appendices

### 2.1 GRIN lens Printing Platform Design

Milestone: - Generate detailed performance specifications and design for a multi-print head microjet printing station having the capabilities needed for printing AGRIN lenses of at least 5" in diameter.

#### 2.1.1 Platform Design Concept

The selected concept involves utilizing multiple print heads containing optical fluids of differing index of refraction to dispense droplets onto a rotating support substrate, as indicated schematically for the key components in **Figure 1**. (The same concept may also be used to fabricate GRIN lenses with low-melting IR-glasses of differing index when print head operational temperatures up to 500°C are achieved). Here the materials are dispensed sequentially from the different print heads mounted on a Z-stage along the X-axis, as the substrate rotates and translates along the X-axis. The substrate translation speed and distance

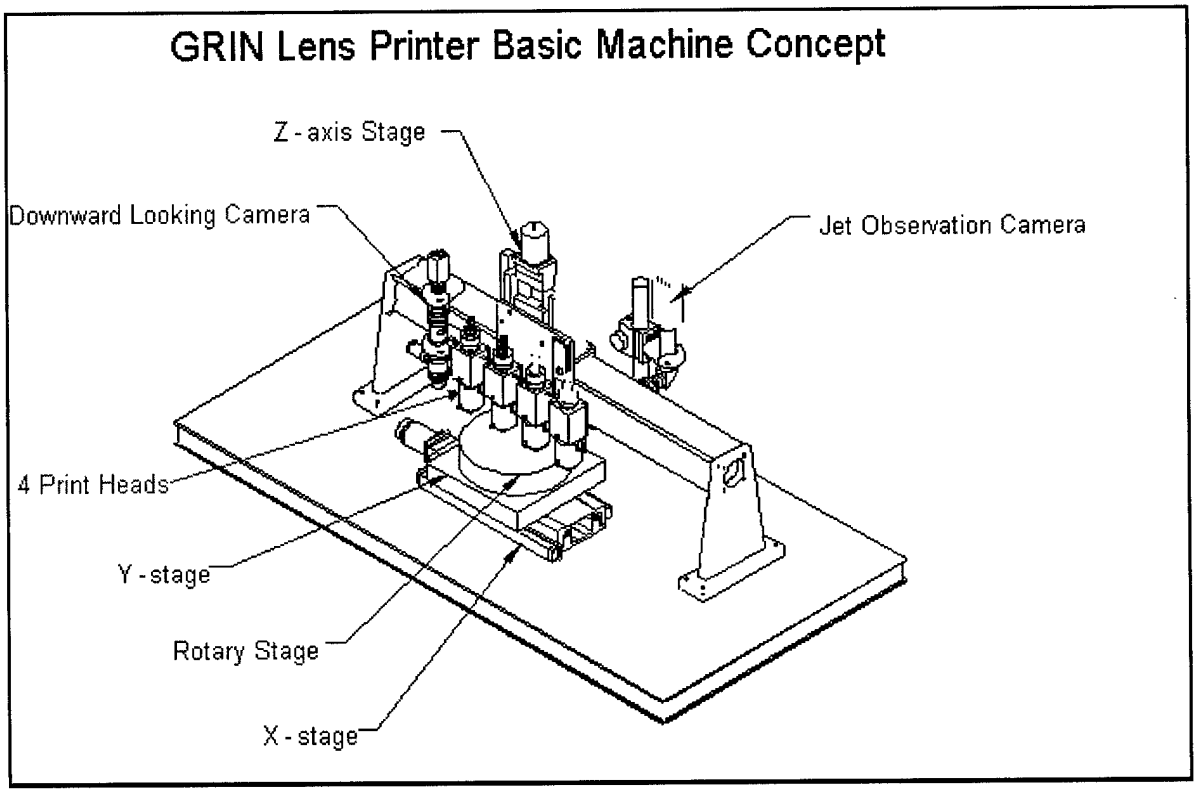


**Figure 1**. *Key component layout for a 4-print-head GRIN lens microjet printer in which fluids of differing refractive index are dispensed onto a rotating glass substrate, with cameras for jet observation and in-situ part inspection.*

along the X-axis are coordinated with the rotational speed to obtain coaxial circular or annular coatings of uniform thickness. The lens is then built up in a layer-by-layer fashion with the print heads being raised along the Z-axis to maintain constant distance between printing device orifice and the lens surface. Here the printing within a layer and from layer-to-layer is driven by "image" data input for each layer entered into the software as CAD file cross-sections developed from optical models. Achieving the requisite amount of inter-diffusion among adjacent deposits of differing materials for smooth gradient profiles will be done by varying the temperature of the substrate with an array of underlying TECs (Thermo-Electric Cooler), briefly heating the still liquid but relatively viscous materials upon completion of each layer. After printing the entire lens it will be solidified in-situ by UV-curing and hardened by post-UV baking. The downward and horizontally oriented cameras are for target-alignment and droplet formation observation, respectively. The coordination of substrate motion with print head elevation, selection and dispensing algorithm are controlled by software, which translates input files into 4-"color" bit maps and provides either fire-on-fly or step-and-print modes of dispensing.

The GRIN Lens Printing Platform layout is indicated in **Figure 2**. The printing enclosure, containing the components of Figure 1 and associated optics, is environmentally controlled, with a laminar flow, Class 100 clean air hood on top and fume exhaust at the bottom. The motion control stages are located on a vibration-insulated table for enhanced printing placement accuracy, and all of the wiring is laid out to meet UL specifications. The adjacent control panel cabinet contains the control PC and the two camera monitors. The software is

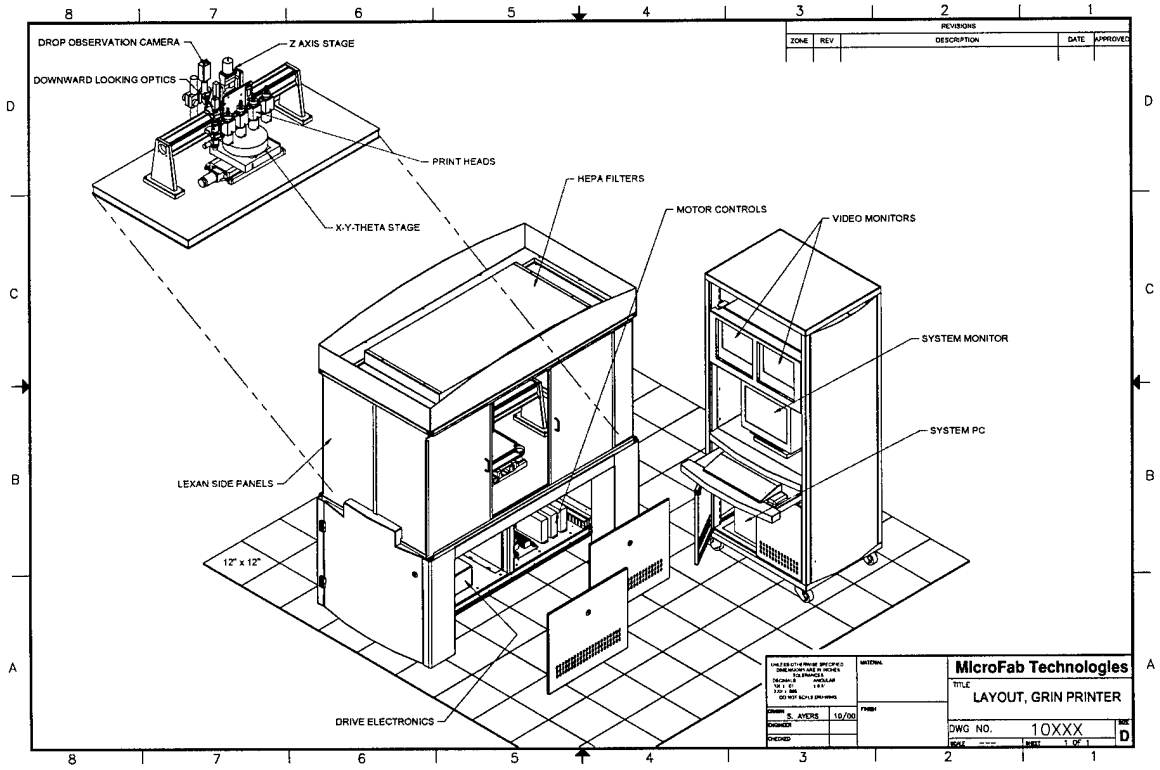


**Figure 2.** *GRIN lens 3D Printing Station Layout.*

entirely menu driven and capable of accepting data from CAD files. A functional block diagram showing relationships among the major subsystems is given in **Figure 3**.

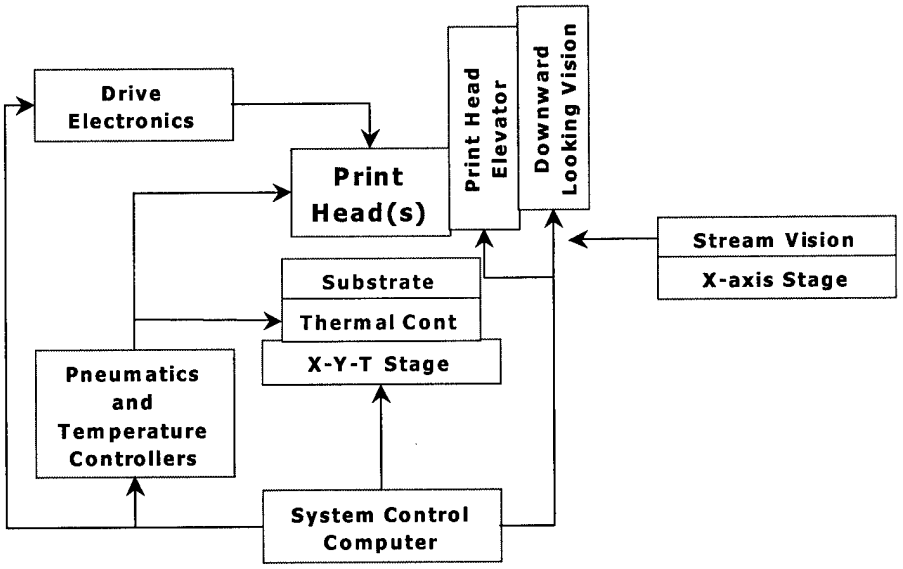


***Figure 3.*** *Block diagram of major subsystems of GRIN Lens Printing Platform providing an overview of machine functionality.*

2.1.2 Design Details

A Bill of Materials for the GRIN Lens Printing Platform, which details parts, components and subsystems by vendor, part # and current price, is given the Appendix (Sec. 4.1). Included are overviews of machine assemblies; listings, by component category, of all of the key electrical, mechanical, pneumatic, vacuum, and optical systems, subsystems and assemblies; and installation/facility specifications.

2.1.3 Motion & Optical Fluid Micro-Dispensing Control

For large lens fabrication the cylindrical or spherical nature of the lens to be created suggests using a rotational stage on top of an X-Y table to create the lens layer by layer in concentric circles. For this only one of the linear axes (X) is needed to vary the radial position of the dispensing device over the substrate (from the point of view of the rotating substrate). The second linear axis (Y) is needed to allow alignment of the rotational axis with the dispensing device. Deposition of the materials of differing refractive index in concentric circular patterns in GRIN lens printing has the advantage of having only the rotational axis in motion during printing, allowing the maximum use of all possible alignment corrections on the linear axis for the highest possible accuracy on spacing between the circles. Specific software-controlled recipes will be developed during Phase-II for coordinating the linear and rotational substrate speeds with the dispensed liquid flow rate so as to allow for the centripetal force and obtain uniform coating thickness on the spinning substrate, while avoiding an anomaly at the very center (where the force is zero). The precise algorithms utilized will depend on a number of factors such as dispensed fluid viscosity and lens diameter and will have to be developed empirically after the platform is built. Avoiding a coating thickness non-uniformity at the center of the lens will be addressed by sequencing of the depositions for each layer, e.g., by making an initial deposit of a number of droplets of fluid at center with the substrate stationary then beginning the deposition of the annular pattern at some distance from the center. Again, we will make sure that the software allows for any arbitrary sequencing of dispensing events as a

function of print axis position on the substrate and determine the optimal process experimentally.

This GRIN Lens Printing Platform may also be used to directly write any number of other types of optical components besides GRIN lenses for a wide variety of applications, such as low-cost microlens arrays of custom configuration and microlenses printed onto GaAs arrays of VCSELs (vertical-cavity surface-emitting laser) and micro-detectors for enhancing optical coupling.

### 2.1.4 Stabilization, Diffusion and Solidification of Deposited Fluids

In order to fabricate lenses having 3D index gradients corresponding to modeled GRIN lenses by the layer-by-layer printing of mosaic patterns of optical materials of differing refractive index, the system must have certain capabilities for controlling the deposited materials. The aspects requiring such control are:

(a) maintaining stability of the relative positions of the deposits of differing inks prior to solidification;

(b) allowing limited inter-diffusion across boundaries between adjacent deposits in order to provide gradient smoothing; and

(c) providing uniformity of solidification and curing of the printed lenses in order to avoid anisotropic shrinkage and density striations and to minimize stresses.

The primary parameter for material stabilization and controlled inter-diffusion will be material viscosity, via control of the temperature. In this design an array of TEC heater/coolers will be mounted between the chuck and rotating stage. To accommodate the rotation two conductive rings will be mounted around the outer edge of the substrate chuck with pick-off electrodes in contact with these rings but mounted on the non-rotating part of the substrate assembly, as indicated in **Figure 4**. However, a similar system for a thermocouple temperature detector may not be viable if the electrical noise generated by the moving contacts is comparable to the low-level dc current levels utilized in a traditional thermocouples. If this turns out to be the case, we will incorporate a remote temperature detection method (e.g., infrared) to provide the feedback to the TEC controllers.

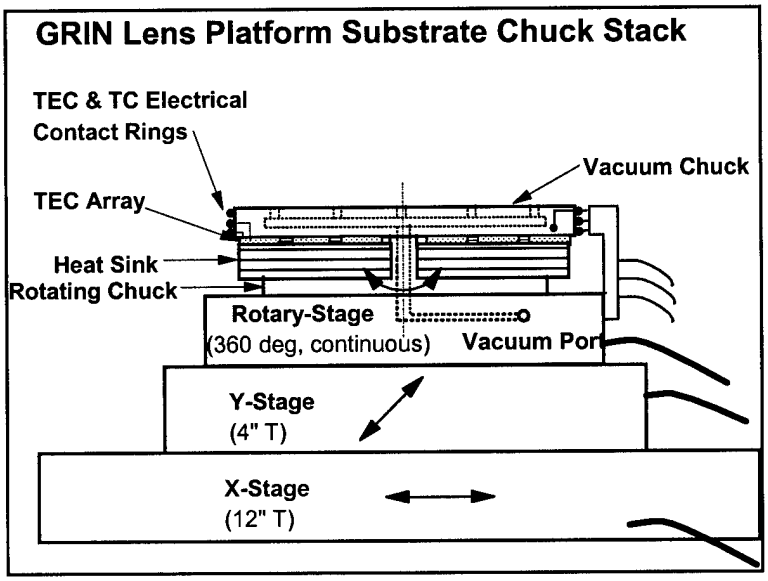


**Figure 4.** *Concept for printing platform substrate chuck indicating control of motion, vacuum and temperature.*

### 2.2.5 Printing from CAD Files of Modeled GRIN Lenses

A key requirement for the GRIN lens printing machine is that it have the capability to be entirely data-driven from files derived from optical models rendered in CAD (computer automated design) format. CAD programs usually save information on objects in vector form or parameterized form. For printing in drop-on-demand mode, this information needs to be discretized. Lens design in a CAD program will generate a representation of the lens in terms of solid, three-dimensional objects (disks, spherical sections, their compliments in a cylinder, and similar geometric features) guided by the requirements of the optical performance without immediate regard for the printing process. One restriction to be observed during the CAD design is the minimal bulk thickness of a layer or shell of material that can be produced by the printing process.

A post-processing step to the CAD design, to be performed wither with the CAD tool or a separate, custom written tool, is to slice the CAD objects into layers that are amenable to printing. Experimentally we will determine what density of droplets is needed to produce the bulk part of such a layer. For the placement of droplets, the layers of the CAD object can then be subdivided into concentric rings with the following criteria:

(a) The center is actually a cylinder with the same volume as the generated droplet;
(b) Each successive ring is divided into a number of equal-volume circumferential sections, i.e., all sections have the same angular extent around the ring;
(c) The number of these sections and radial extent of the ring are optimized to produce, in the plane of the layer, cross sectional areas with diagonals intersecting as close to a right angle as possible, given the predetermined volume.

This problem can be solved with standard numerical optimization techniques.

From the software perspective a convenient format to use in going from modeled lens design to automatic control of platform functions in GRIN lens printing is AutoDesk's DXF data format, popularized through their high-end AutoCad design program. The DXF files contain information in ASCII text format and are thus easily read. The challenge here is to identify all logical elements that may appear in this file for the project at hand and devise a suitable discretization algorithm. This type of exercise has been done before. A recent example involving discretization for the purpose of drop-on-demand printing from CAD designs has been reported by a group of Nagoya University in Japan (K. Yamaguchi et al., Prec. Eng. 24 (2000) 2-8). Detail issues to be addressed during Phase-2 include where to do the slicing into layers (CAD program writing DXF files, or custom converter reading DXF files), how to keep track of material assignments to elements, and what printing strategies to use.

### 2.1.6 Maximizing GRIN Lens Printing Throughput Rates

Ink-jet printing systems typically dispense droplets of fluid of diameter over the range 30-50 μm (micromillimeters) and in volume from about 14 to 65 picoliters ($10^{-12}$ liters). Since the anticipated volume for a 6" diameter GRIN lens fabricated by this machine will be on the order of 0.08 liters ($8x10^{10}$ picoliters), the goal will be to achieve fluid flow rates which will

enable the printing of such a large lens in just a few hours (verses several days). To achieve this goal we will pursue several approaches in parallel. The first will be to maximize the volume of droplet which can be dispensed by our printing devices, and we believe that ink-jet dispensing of droplets of up to 200+ picoliters may be achieved with our current technology. The second approach will be to utilize existing software which enables the firing of bursts of droplets in the print-on-the-fly mode, versus the step-and-print mode, whereby the net flow rate of droplets onto the substrate will be on the order of 5,000 drops/sec, with maximization of both the dispensing frequency and the speed of the motion controller. A third approach which will be investigated in Phase-2 work will be the use of multiple-jet or array print heads for each of the different fluids being printed.

## 2.2 Materials System Development

Milestone: - Establish and verify experimental procedures for the development of a set of optical quality formulations which are required to print large GRIN lenses of correct optical performance.

### 2.2.1 Visible-to-Near-Infrared Optical Materials System

Any optical material system utilized for ink-jet printing of lenses must meet two general criteria. Firstly, it must be formulatable as fluid with the rheology required for dispensing by the ink-jet printing method and, ideally, be 100% solids to avoid anisotropic shrinkage upon solidification. To be dispensed by the "drop-on demand" printing method any fluid must be reducible in viscosity, by heating in the case of 100% solids formulations, to below the 30-40 centipoise level. Secondly, it must exhibit, upon solidification & curing, those particular properties requisite for the intended application, such as optical transparency at the wavelength of interest and sufficient chemical, thermal and mechanical durability. Thermoplastics, often used in free-form rapid prototyping 3D printers, may be formulated with good optical transparency in the visible and near IR (infrared) wavelengths but those with flow temperatures low enough for ink-jet printing (<100°C) would be too thermally unstable for this application. Accordingly, we came to the conclusion that the most suitable optical material system meeting both the current printing and the application sets of requirements would be UV (ultra-violate)-curing optical epoxies.

UV-curing reactive pre-polymer fluids were prepared and utilized for experimental printing of test grin lenses using MicroFab's current dual-head optics printing station. These pre-polymers were all-organic fluid systems that are UV reactive and cure to form amorphous optical quality plastic, which can be in the form of a lens when ink jet deposited. The organic oligomers and monomers that compose the fluids were both mono-functional and poly-functional containing reactive epoxide, hydroxyl, and vinyl ether groups. Higher refractive indices of the resulting plastic lenses were produced by having higher aromatic content in the basic organic structures, and conversely, lower refractive indices resulted from a greater aliphatic or cyclo-aliphatic content.

The primary technical challenges in developing on optimum UV-curing optical epoxy material system at this stage of development were twofold: control of the mutual solubility of all constituents of the combined fluid systems; and, adjustment of the fluids' refractive indices to achieve the short term goal. Obviously, each fluid must have mutual solubility of all its components. Beyond that, all of the fluids being used to form the grin lens must be soluble in each other in both the fluid and polymerized states, or an amorphous plastic lens will not result from the patterned ink jet deposition of the fluids one with the other. The viscosities of both fluids are a secondary consideration, as this property of each one can effect the diffusion characteristics of the printed lens that will be a combination of all the fluids. The system's tolerance to viscosity differential while achieving the desired refractive index gradient is not well understood at this time, but will be studied further during the course of the Phase-2 work.

The result of the materials development efforts of the Phase-1 work were two optimized and rheologically compatible formulations, MRX-102C and MRX-120A, which were printed at temperatures of 100°C and 150°C, respectively, as dictated by the viscosities of the fluids. The refractive index of the higher viscosity material (MRX-120A) was significantly higher than that of the lower viscosity one (MRX-102C), as was demonstrated in their use in printing GRIN microlenses (Sec.2.3). Additionally, in both formulations the uniformity of UV-curing in bulk structures was experimentally confirmed.

### 2.2.2 Infrared Optical Material System

MicroFab's current printing devices can dispense fluids at temperatures up to nearly 300°C, which is more than adequate for the printing of the optical epoxies developed to date which are transparent from the visible into the near-UV portions of the spectrum. However, there is a class of low-melting- point UV-glasses with transparency into the mid IR which could be used in GRIN lens printing with this printing station when we reach an ongoing goal of extending maximum printing temperature to 500°C. These glasses include, for example, $As_2S_3$ which exhibits good transparency (absorption coefficient less than 0.02 $cm^{-1}$) over the wavelength range 1-8 μm. This glass has a softening point of 208°C, and data we took of viscosity as a function temperature indicated that it should be ink-jet printable somewhere between 500°C & 600°C.

## 2.3 GRIN Lens Printing Process Development

Milestone: - Develop solutions for primary technical challenges in GRIN lens printing and process control and print & characterize small-scale GRIN lenses.

### 2.3.1 GRIN Lens Printing Process Concept Development

*(1) Material Dispensing Algorithms*:

The dispensing process concepts for utilizing this GRIN Lens Printing Station with its rotating chuck in the fabrication of large GRIN lenses are illustrated for the axial and radial GRIN lens cases in **Figures 5 and 6 & 7**, respectively. In both cases the X-axis of the chuck containing the support substrate moves sequentially beneath the print heads containing the fluids

of differing refractive index and rotates and translates in the X-direction to deposit an annular layer of material coaxial with the center of the chuck in a layer-by-layer fashion, as indicated. The degree of lens curvature achieved naturally during printing by the cohesion and surface tension forces of the materials in the liquid state may be controlled by treatment of the supporting substrate with a non-wet (low surface energy) coating around the periphery of the lens.

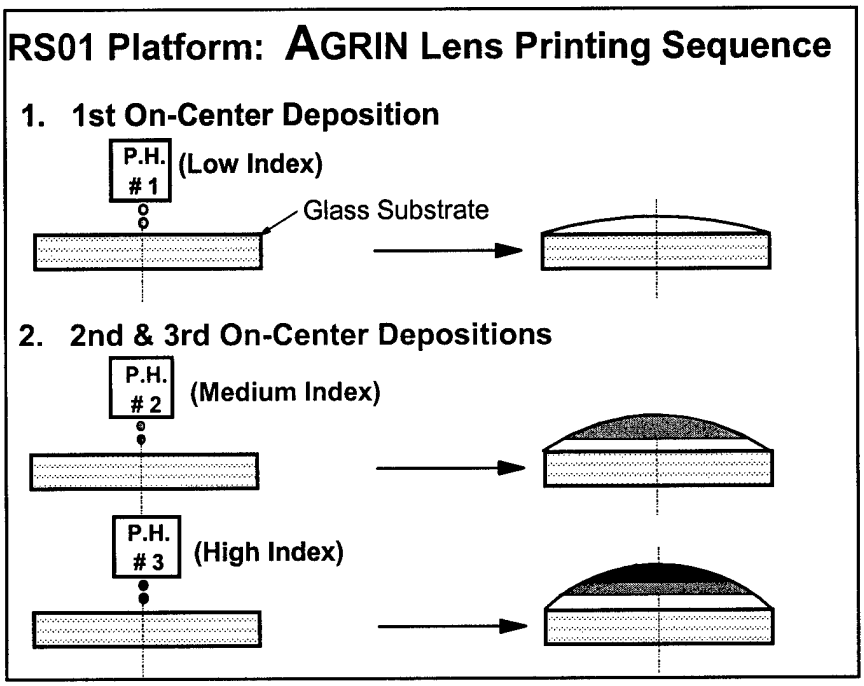


**Figure 5.** *Concept for printing axial gradient index of refraction lens using three fluids of differing refractive index.*

*(2) Controlling Inter-diffusion between Adjacently Printed Materials of Differing Index:*

The optical fluids developed for GRIN lens printing must be mutually miscible, despite the fact that they will be formulated to span a rather wide range in refractive index, in order to enable the formation of smooth (versus step) index gradient profiles. However, the degree of inter-diffusion must be tightly controllable to enable maintaining the designed gradient profiles in multi-fluid printed layers, and from layer to layer, prior to solidification. We plan to address this challenge by varying the temperature of the printed fluids on the substrate, keeping the

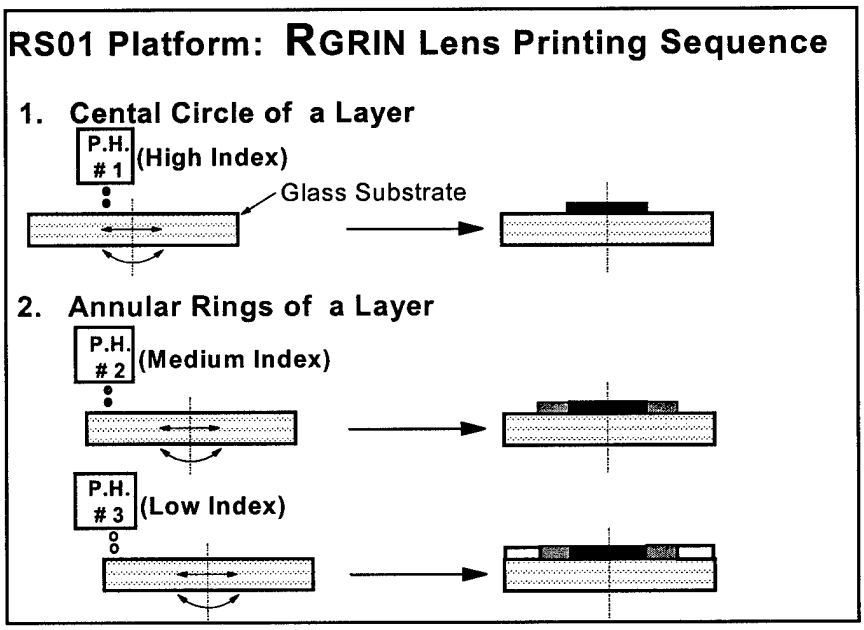


**Figure 6..** *Concept for printing radial gradient index of refraction lens using 3 optical fluids of differing refractive index.*

substrate somewhat below room temperature during each printing sequence, in order to maximize viscosity and inhibit inter-diffusion, except for brief periods of heating above room temperature to smooth out boundaries.

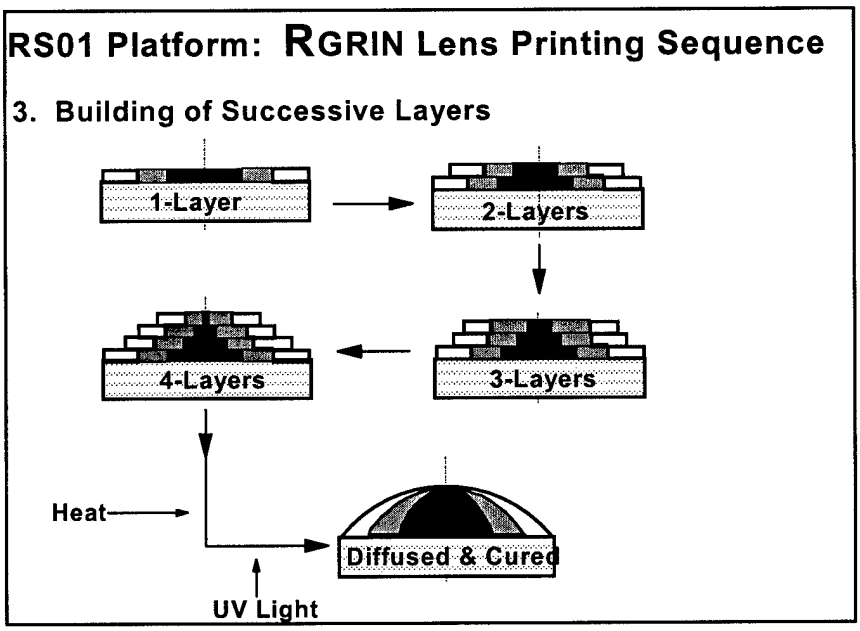


**Figure 7.** *Concept for printing a radial index of refraction lens using 3 optical fluids of differing refractive index.*

*(3) Obtaining Uniformity of Cure throughout the Printed Lens:*

In-situ cures of the lens structure during fabrication, e.g., after printing each layer, would facilitate maintenance of structural stability during the lens fabrication process. However, we have found that it is difficult to avoid creation of a "skin" of higher density material at the surface exposed to the UV-input. Such density anomalies, if located at various levels below the surface of a lens, can scatter transmitted light. Consequently, we have developed a process for post-print curing of the lenses which will enable achievement of a uniform cure throughout the volumes of lenses at least 1/8" thick. The strategy developed for doing this is based both on well known approaches for UV-curing of such materials and on experiments performed during the Phase-1 work period. Since the longer UV wavelengths, e.g., 300-400 nm (nanometers), are capable of deeper penetration into pre-polymeric fluids than the shorter ones (<300 nm), UV-curing begins by relatively long (1 ½ hrs) exposures to a low-intensity (<0.1 Watt/cm$^2$), "black-light" which typically cuts off just below 300 nm. This initiates the UV-curing process chemically when bonds of the photo-initiator molecules are broken by absorption of photons, releasing the free radicals that diffuse through the material over time and promote the formation and cross linking of monomer chains. The low intensity UV-exposure is then followed by baking the lens at 100°C for an hour or two to drive out water vapor which would inhibit free radical diffusion. Finally, the hardness of the surface of the lens is exposed to UV-irradiation containing wavelengths down to 200 nm from a high-intensity (1-2 Watt/cm$^2$) source. The effectiveness of this process for obtaining highly uniform curing in bulk structures composed of these prepolymer formulations was confirmed by the imaging qualities achieved with lenses up to 1/8" in thickness printed onto glass slides. Additional confirmation will be obtained during Phase-2 by SEM (scanning electron microscope analysis of cross-sections of printed macrolenses.

2.3.2 Small GRIN Lens Printing Experiments

The high and low index formulations of optical epoxy prepolymers, MRX-120A and MRX-102C, respectively were used in our dual-print-head, R&D Optics Printing Station to print microlenses up to 1 mm in diameter, in order to study materials interactions verify certain process concepts to be utilized in the GRIN Lens Printing Platform designed here. As the first experiment, a series of microlenses with diameters ranging from 150 to 800 μm, as exemplified by the micrograph of **Figure 8**, was printed onto a low-wet-treated-glass substrate with each fluid. The back focal length of each lenslet was determined using an inverted microscope at 100X magnification with white light from the lenslet side to measure the distance between the top substrate surface and the plane at which the edges of the incoming light aperture came into clearest focus within the substrate, then subtracting the microlens thickness obtained from profile measurement.

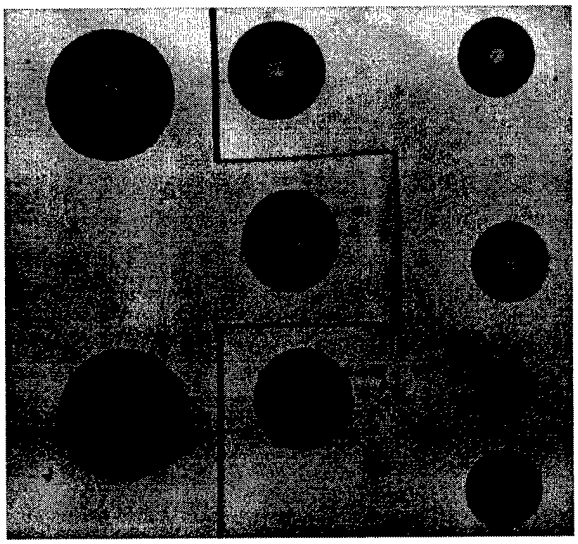

**Figure 8**. *Photo at 40X magnification of microlenses printed with 200, 100 & 50 each (left-to-right) droplets of MRX-102 optical epoxy.*

The difference in refractive index for these two fluids was confirmed by the data for focal length as a function of diameter. As can be seen in **Figure 9**, the higher index material provides, as expected, both a shorter focal length at the same lenslet diameter and a lower f-number (f/# = focal-length/diameter).

Direct measurement of the refractive indexes of these lens materials in the cured state would require spinning thin (6-9 μm) films of solvent-diluted versions of the formulations onto $SiO_2$ -coated silicon wafers, curing the films then coupling single-mode light into the planar waveguides formed in this fashion. We did not have at hand the light-generation, coupling and measurement equipment to do this direct measurement. In theory, however, the indexes of the two materials may be calculated from measurements of the diameters, focal lengths and heights of these microlenses. First, from microscopic

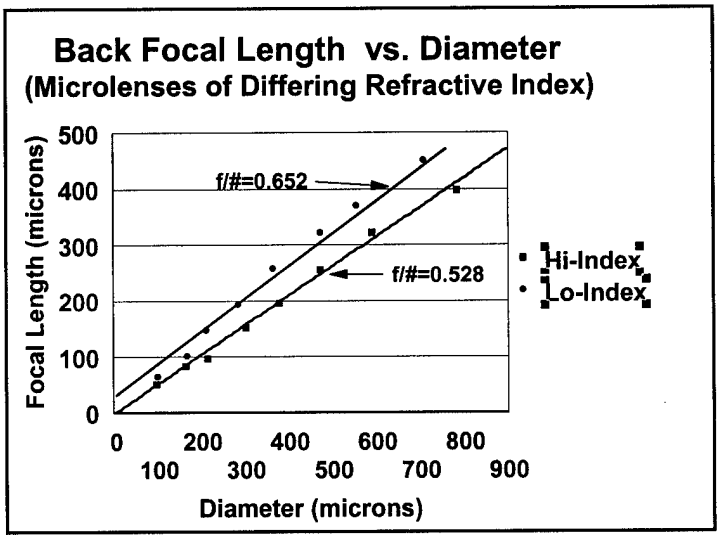


**Figure 9.** *Back focal length as function of diameter for microlenses with two differing index of refraction fluids, showing lower focal lengths at same diameters and lower f/#s (slope) for higher index material.*

measurements of the diameter, $D$, and height, $h$, (in profile) a radius of curvature, $R$, for each of the lenses of Figure 7 was calculated according to the formula:

$$R = \{ [h^2 + (D/2)^2] / [2xH] \}$$

In the thin lens approximation the refractive indexes, $n$, of the lens materials may be calculated from their focal lengths, $F$, (in air) and radii of curvature, $R$, as follows:

$$F = R/(n-1)$$

$$n = 1 + R/F$$

The index of each material at the white-light microscope wavelengths may then be calculated, within the limits of the approximation formula, from the slopes of the best linear fitting curves of the plot of focal length versus radius of curvature, as shown in **Figure 10**, as:

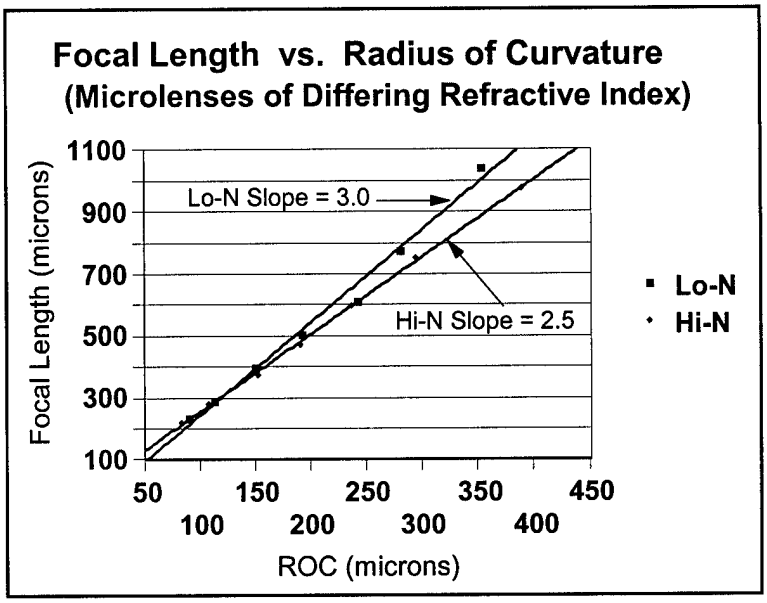


**Figure 10.** *Focal length in air as a function of lens radius of curvature (ROC) for microlenses printed with optical materials of differing index (N), which provides index values from the inverted slopes of the best-fit lines.*

n(low) = 1.333

n(high) = 1.400

$\Delta n = 0.067$

These index values calculated from lenslet focal length and geometric data are lower than we believe them to be in actuality, due to the approximations used in the calculations, but the resulting index difference between the two formulations appears to be close to the expected value.

After confirming the difference in index of refraction between the two optical materials our dual print head system was used to print axial GRIN lenses by depositing varying numbers of droplets of the higher index fluid directly on top of deposits of the lower index one. After deposition of the second material the lenslets were allowed to inter-diffuse for 5 minutes prior to solidifying the compound structures with UV irradiation. The droplets produced by both print heads were adjusted to be about 51 μm in diameter, so the volumetric content of one material could objective of these experiments was to try to determine, to first order, the volumetric ratio which produced the largest and index gradients within the lenslets, as determined by focal length

data. In **Figure 11** such data are presented for two lenslet series of volume differing by a factor-of-two. If the two materials were completely inter-diffusing into each other in the time allowed before solidification one would expect to see a relatively smooth reduction in focal length as this averaged index value changes from that of the lower index material (0%) to that of the higher index one (100%). In both cases, however, one sees a significant deviation from the homogeneous index case for the 20%-high-index/80%-low-index lens composition, in the form of a precipitous drop in focal length. The fact that this phenomena appears to be identical in lenslets of differing size strongly suggests that a significant axial index gradient has been created with this particular composition of materials and at the inter-diffusion time selected. Such a result would be confirmed if future measurements of focal spot sizes also revealed a reduction in this parameter at that composition.

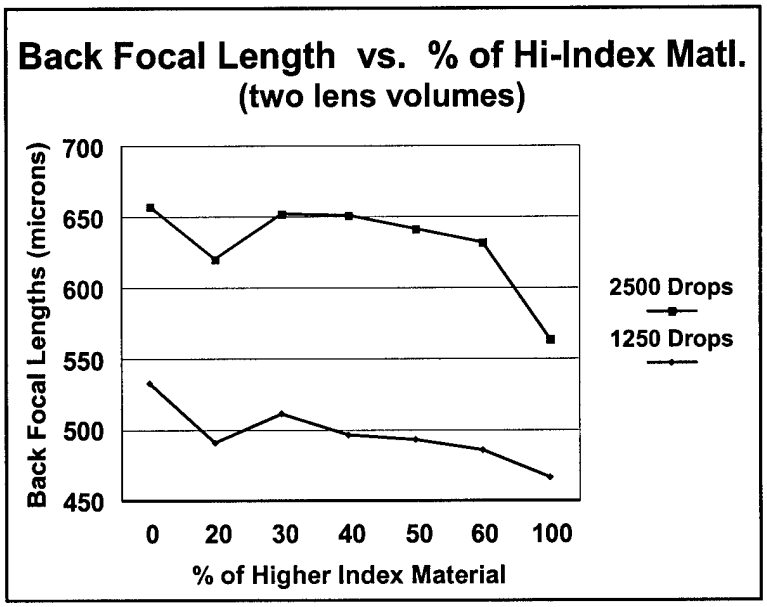


**Figure 11.** *Back focal length of microlenses double-printed with optical fluids of differing index of refraction as a function of percentage of the higher index formulation, for two lenslet volumes expressed in terms of total numbers of 50 μm diameter droplets.*

We plan to continue the two-component microlens printing experiments initiated during this Phase-1 work under internal funding and to publish the results in a paper to be presented next year at the SPIE Photonics West Conference in San Jose.

## 2.4 GRIN Lens Design, Modeling and Performance Characterization

Milestone: - Develop designs and models of GRIN lenses for fabrication by layered 3D printing and characterize optical performance of small, printed GRIN lenses.

### 2.4.1 Radial GRIN Lens Modeling

Utilizing the our newly upgraded optical modeling software package (ZEMAX-EE, version 9.0 Engineering Edition), we have studied the effects on optical performance of a theoretical 5" diameter RGRIN lens as a function of both total spread in index of refraction within the lens and lens thickness. The radial index of refraction gradient profiles for this lens with two values of index spread, 0.1 & 0.2, are shown in **Figure 12**. The details of this modeling study are given in the Appendix (Sec. 4.2), but the key conclusions, some of which are not immediately intuitive, may be stated as follows:

As either lens thickness or total spread in refractive index within an RGRIN lens increases:

(a) Focal length decreases;

(b) Focal spot size increases; and

(c) Imaging quality decreases (as measured by the "Strehl Ratio" which reflects the degree of image contrast resolution).

From these results it can be seen that the ideal design selected for a RGRIN lens will depend heavily on its intended application. For example, a thinner lens with smaller index spread would be preferred for high-resolution imaging of target objects at relatively large focal distances, whereas a thicker lens with larger index spread would be preferred for collection of optical power from a source and focusing it into a detector.

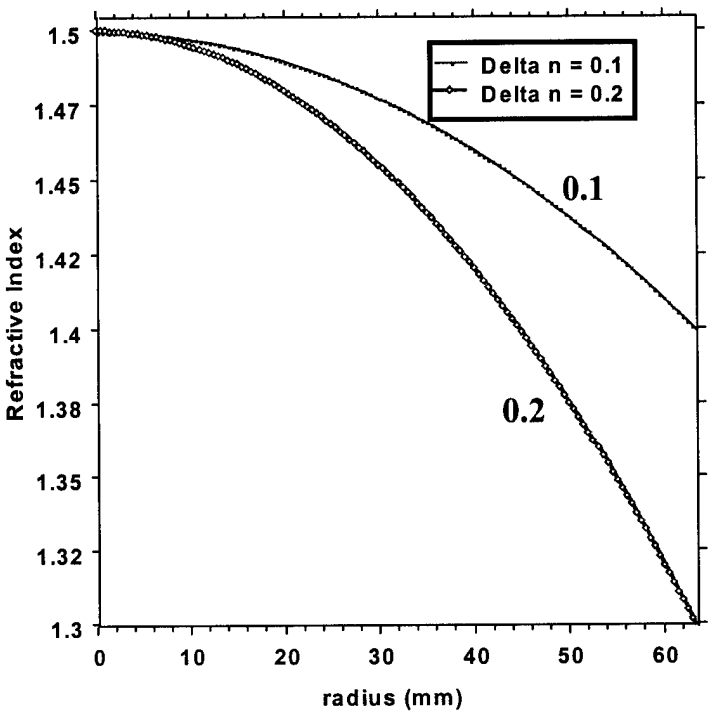


**Figure 12.** *Refractive index versus radial position for two 5 inch diameter RGRIN (radial gradient index of refraction) lenses having total index spread of 0.1 and 0.2.*

## 2.4.2 Axial GRIN Lens Modeling

An example of a simulated 3D model of the point spread distribution in focused power for lenses of the same physical size which was generated by the Zemax software is given in **Figure 13.** From these data it may be calculated that an axial index gradient of 0.1/mm can provide a ten-fold increase in optical imaging quality.

## 2.4.3 Printed GRIN Lens Characterization

We have shown in Section 2.3.2 above that approximate refractive index data may be obtained for printed homogeneous-index microlenses by microscopic measurement of diameters, heights and focal lengths for series of lenslets of differing diameter. We have also demonstrated (Figure 10) how the volumetric ratio of two fluids of differing refractive index used to print axial GRIN microlenses may be adjusted to optimize the index gradient profile. The imaging performance of a lens may also be determined very quantitatively by measuring the power distribution in the focal plane, as illustrated in the 1D, 2D and 3D profiles shown in **Figure 13**, where the width of the power peak at the half-maximum level indicates the level of aberrations present.

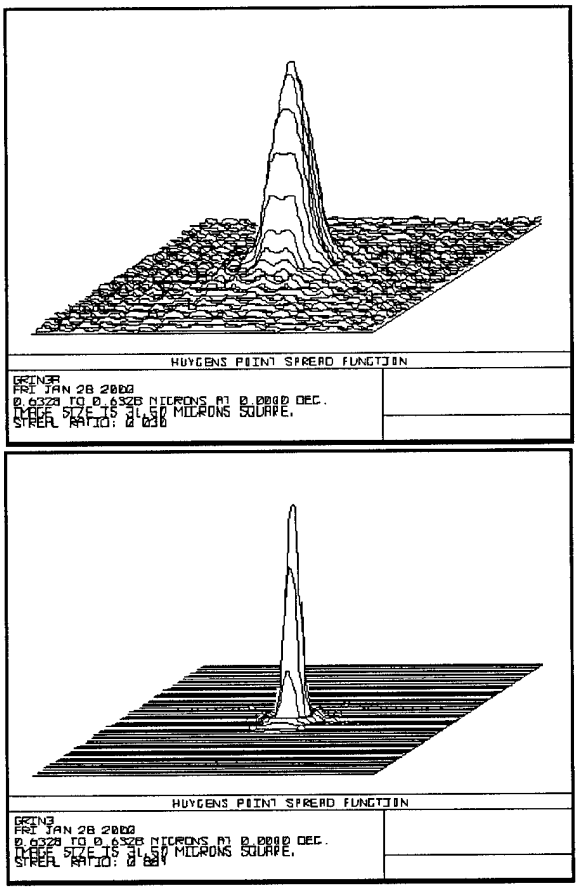


***Figure 13*** *Calculated point spread functions for homogeneous (top) and axial GRIN (bottom) lens of same geometry, where GRIN lens index gradient is 0.01 per 50 μm of height.*

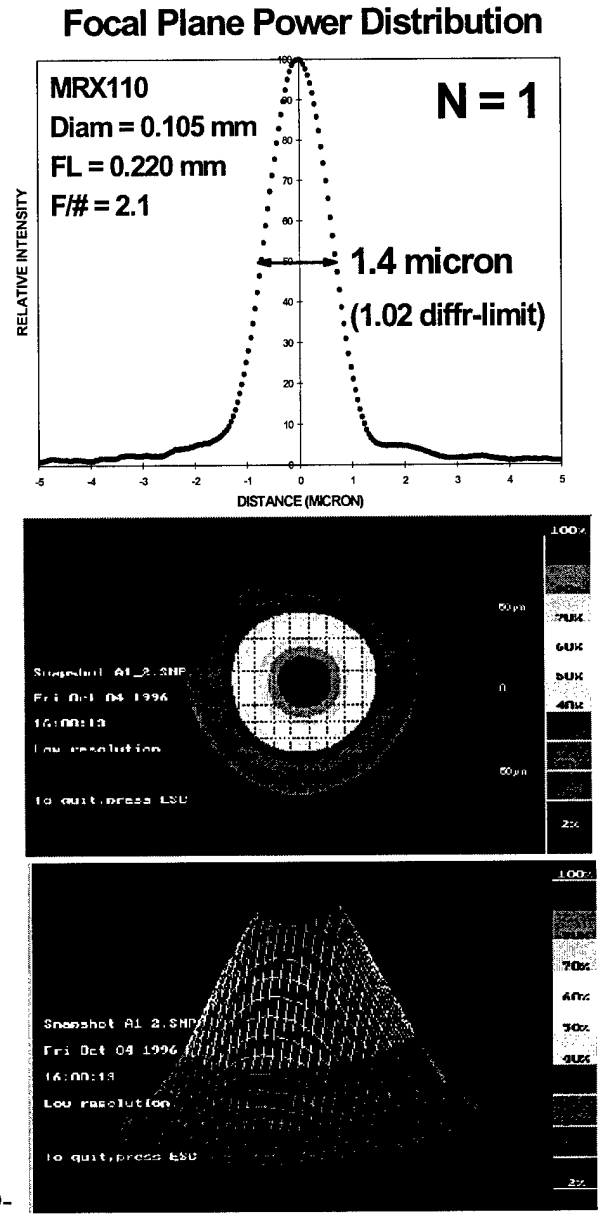


***Figure 14.*** *Examples of 1D, 2D and simulated 3D distributions in focal plane power for a lens under test with beam analyzer system.*

## 3.0 Conclusions

It may be concluded from the Phase-1 work that the printing of GRIN lenses from CAD-file data derived from models, using a 3D ink-jet printer concept with optical prepolymer, UV-curing epoxy formulations (and, ultimately, with IR glasses) of differing refractive index, is quite feasible. The machine design developed, along with the printing processes conceptualized and partially verified by small lens printing, should greatly facilitate success with a Phase-2 effort to build and demonstrate a commercializable GRIN Lens Printing Platform for reproducible, rapid-prototyping/manufacturing of both gradient and homogeneous index of refraction lenses up to six inches in diameter and with good optical quality.

# 4.0 Itemized Man-Hours and Costs

| Internal Man-Hours & Cost By Task | | | | | | | |
|---|---|---|---|---|---|---|---|
| April 27, 2000 thru December 31, 2000 | | | | | | | |
| **Task A** | | **April 27 thru July 31** | | | **August 1 thru December 31** | | |
| Employee | Title | Hours | Cost | Cum | Hours | Cost | Cum |
| | | | | | | | |
| Scott Ayers | Principal Engineer | | | | | | |
| Hans -Jochen Trost | Senior Scientist | | | | | | |
| Steve Karcher | Mechanical Designer | | | | | | |
| W.R. Cox | Principal Scientist | | | | | | |
| Don Hayes | Principal Scientist | | | | | | |
| David Wallace | Principal Scientist | | | | | | |
| | | 122 | 5,591.60 | | 252 | 11,797.65 | |
| Fringe @ 33.% | | | 1,845.23 | | | 3,893.22 | |
| Labor OH @ 30% | | | 1,677.48 | | | 3,539.30 | |
| G&A @ 10.50.% | | | 986.06 | 9391.01 | | 1,238.75 | 20,651.73 |
| Other Direct Cost : | Equipment /Supplies | | 276.70 | | | 1,421.56 | |
| | | | | | | | |
| | | | 10,377.06 | | | 21,890.48 | |
| Fee @ 5% | | | 518.85 | | | 1,094.52 | |
| | | | **10,895.92** | | | **22,985.01** | |
| | | | | | | | |
| | | | | | | | |
| **Task B** | | | | | | | |
| W.R. Cox | Principal Scientist | 32.5 | 1,446.71 | | 92.5 | 4228.11 | |
| | | | | | | | |
| Fringe @ 33.% | | | 477.41 | | | 1,395.28 | |
| labor OH @ 30% | | | 434.01 | | | 1,268.43 | |
| G&A @ 10.50% | | | 247.60 | 2,358.14 | | 2,599.85 | 6,891.82 |
| | | | 2,605.74 | | | 9,491.67 | |
| Fee @ 5% | | | 130.29 | | | 474.58 | |
| | | | **2,736.03** | | | **9,966.25** | |
| | | | | | | | |
| | | | | | | | |
| **Task C** | | | | | | | |
| Quiang LU | Senior Scientist | | | | | | |
| W.R. Cox | Principal Scientist | | | | | | |
| Rick Hoenigman | Print Test Engineer | | | | | | |
| Tracy Cui | Assemble Tech. | | | | | | |
| Aihua Zhao | Assemble Tech. | 186.5 | 4,060.41 | | 532.5 | 12,595.79 | |
| | | | | | | | |
| Fringe @ 33.% | | | 1,339.94 | | | 4,156.61 | |
| Labor OH 30% | | | 1,218.12 | | | 3,778.74 | |
| G&A @ 10.50.% | | | 694.94 | 6,618.47 | | 1,322.56 | 20,531.14 |

| | | | | | | | |
|---|---|---|---|---|---|---|---|
| | | | 7,313.41 | | | 21,853.70 | |
| Fee @ 5% | | | 365.67 | | | 1,092.68 | |
| | | | **7,679.08** | | | **22,946.38** | |
| | | | | | | | |
| **Task D** | | | | | | | |
| Chi Guan | Optical engineer | 247 | 4,392.05 | | 62 | 1,027.96 | |
| | | | | | | | |
| Fringe @ 33.% | | | 1,449.38 | | | 339.23 | |
| Labor OH 30% | | | 1,317.62 | | | 308.39 | 1,675.57 |
| G&A @ 10.50.% | | | 751.70 | 7,159.04 | | 107.94 | |
| | | | 7,910.74 | | | 1,783.51 | |
| Fee @ 5% | | | 395.54 | | | 89.18 | |
| | | | **8,306.28** | | | **1,872.69** | |
| | | | | | | | |
| | | | | | | | |
| | | 588 | 29,617.30 | | 939 | 57,770.32 | |
| | | | | | | | |
| | | | | | | | |
| | **Total** | **1,527** | **87,387.62** | | | | |
| | | | | | | | |
| | **Funds Remaining** | | **10, 655.38** | | | | |
| | **(as of December 31,2000)** | | | | | | |

# 5.0 Appendices

## 5.1 GRIN Lens Printing Platform Specification & Design

### 5.1.1 Equipment Overview

A. Purpose/Function:

– The gradient index of refraction (GRIN) printing platform has been designed to support the ink jet deposition of various optical epoxy materials used in the formation of a GRIN lens.

B. Basic System Structures/Features:

– The major subsystems of the printing platform are:
(1) Jetting subsystem
(2) X-Y-Z-Θ positioning system
(3) Table / machine base
(4) Jet observations optics
(5) Target vision system

C. Conceptual Overview of Design:

(1) Schematic representations of the GRIN Lens Printing Station key components, layout, and system overview showing the relationships between major machine functions have already been given in Figures 1-3.
(2) Basic theory of operation – The machine will provide automated functionality, while using manual material loading and adjustment of parameters. Patterns will be printed radially and in layers.
(3) System flow charts – Normal machine sequencing is described in **Figure 15**.

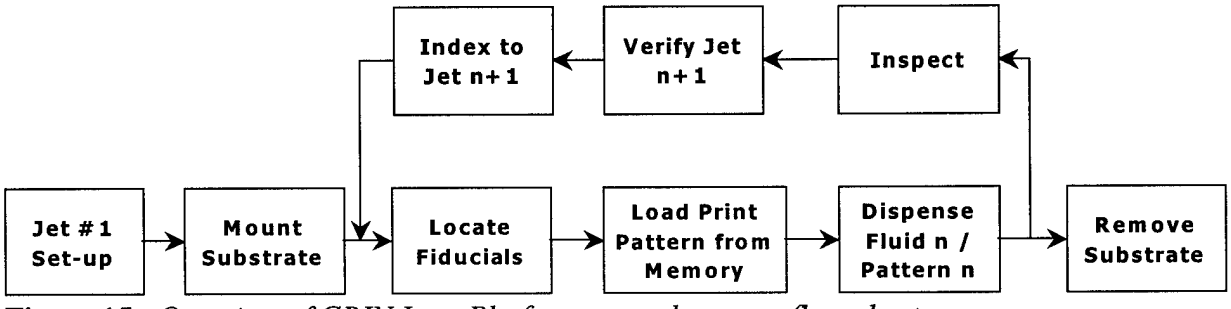


**Figure 15.** *Overview of GRIN Lens Platform normal process flow chart.*

D. Safety:

(1) Overview of equipment-specific safety hazards – The printing platform will be designed to present no specific safety hazards to the investigator accustomed to working in a laboratory environment.

(2) Identification of functional hazards/precautions – Electrical, mechanical, thermal, and chemical hazards will be identified and marked with appropriate warning labels as required.

(3) Lockout/tagout procedures and information – Main power to the machine is routed through a switch located on the right front leg of the machine. This switch will be compatible with Lockout/tagout procedures.

(4) Certification by United Laboratories is anticipated.

E. Facilities Requirements:

(1) Floor space requirements – The machine will be installed in an area which is 13' wide, 11' deep and a minimum ceiling height of 8'.

(2) Air conditioning/ventilation/environmental requirements: – Equipment temperature rise and air replenishment requirements TBD.

(3) Floor loading – The main unit will be approximately 1000 lbs., with leveling pads in each corner. The secondary unit will weigh less than 100 lbs.

(4) Electrical – Power outlet at 110VAC and 15 Amps.

(5) Vacuum/pneumatic – The machine will require clean, compressed air regulated to 100 PSIG. Vacuum to be provided at 25 in Hg.

(6) Process/special gases – None required for base machine operation

(7) Exhaust - TBD; Drains – None required; Other - TBD

### 5.1.2 Machine Assemblies

A. Overview of machine assemblies

(1) Functional block diagrams – a block diagram of major machine components is shown in **Figure 16.**

B. Electrical systems

All identifier symbols in this section refer to the symbols in Figure 16.

(1) DC systems:

(a) E5 – Waveform Generator – Source of the wave form pulse used to actuate the PZT element internal to the jetting device. This unit may be purchased either internal to MicroFab, or from an external commercial source.

(b) E6 – Voltage Amplifier – Used to increase the amplitude of the pulses generated by the waveform generator (E5). This unit may be purchased either internal to MicroFab, or from an external commercial source.

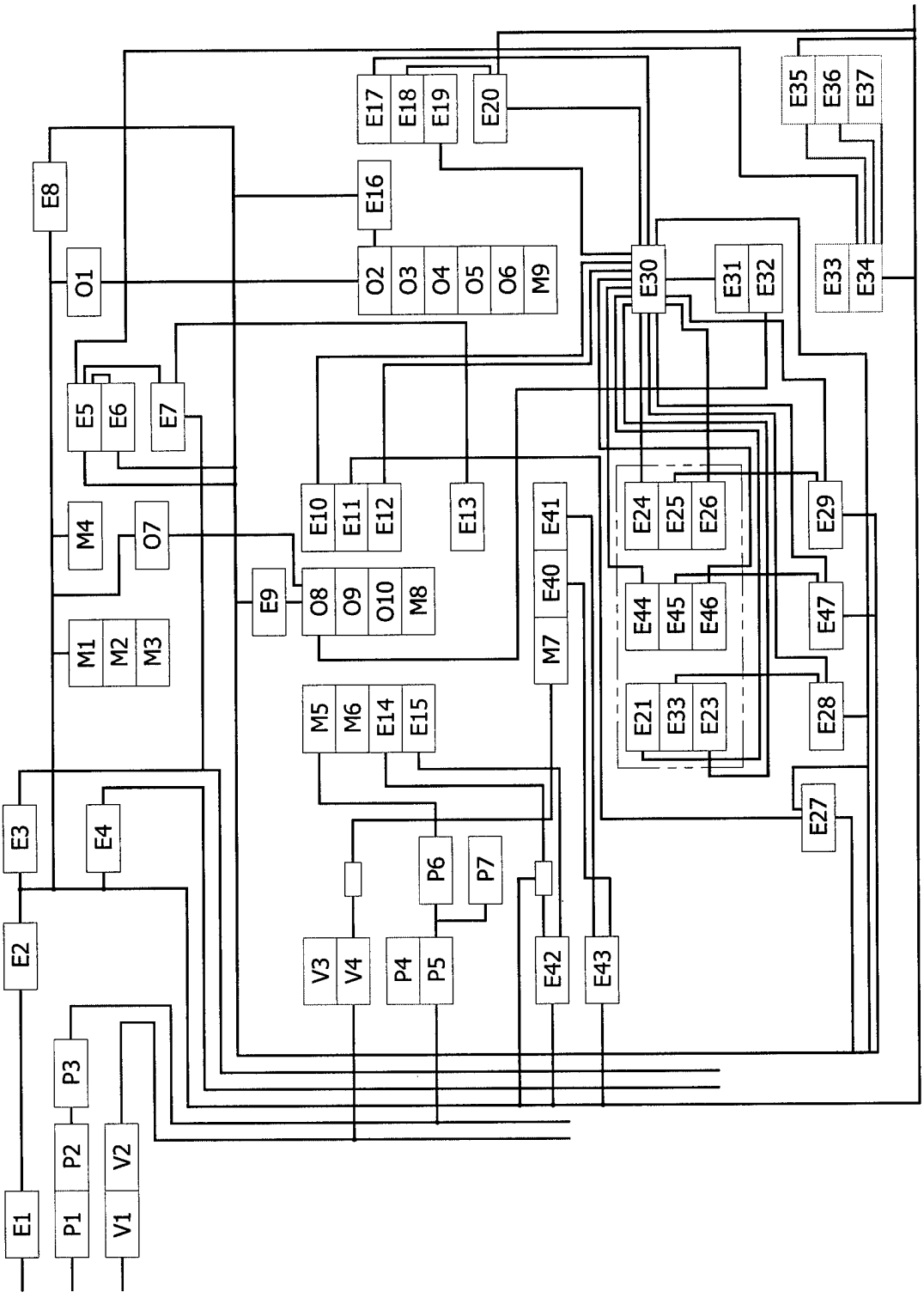


**Figure 16.** *Block diagram of major components of GRIN Lens Printing Platform.*

(c) E7 – Strobe Interface Box – Used to provide a variable delay between the PZT drive pulse and the signal pulse to the strobing LED for jet observation.

(d) E10 – Z-axis Stage with limit switch – Provides 4" travel for the controlled altitude of the jetting device above the targeted substrate.

(e) E11, E18, E25, E33, E45 – Stepper motors – Drive motors for each axis of motion in the machine.

(f) E12, E19, E23, E26, E46 – Digital encoders – Provide positional feedback for each axis of motion in the machine.

(g) E13 – Strobe LED – LED used to provide back lighting to the dispensed droplet for observation by the optics system.

(h) E15 – Thermocouple – Provides temperature read-out of the jet operating temperature.

(i) E17 – X2-axis Stage with limit switch – Provides 8" travel of the drop formation camera along the X-axis.

(j) E21 – X-axis Stage with limit switch – Provides at least 12" of travel along the X-axis for the target substrate.

(k) E24 – Theta Stage with limit switch – Provides continuous rotation of the target substrate

(l) E41 – Provides temperature feedback for the substrate mounting plate.

(m) E44 – Y-axis Stage with limit switch – Provides small Y axis adjustments of the Theta stage to assure that the rotation is directly beneath the print heads.

(2) AC systems:

(a) E1 – Power conditioner (optional) – Purchased component used to stabilize and eliminate noise on incoming machine power.

(b) E2 – Main switch – Controls all 110 VAC power to the machine.

(c) E8 – Emergency Stop – Two switches mounted at the front face of the machine to stop movement of the positioning equipment in the event of an operator's intervention.

(d) E14 – Heating element – Standard heating cartridge for elevating the operating temperature of a viscous fluid.

(e) E20, E27, E28, E29, and E47 – Motor drivers - Commercially available motor controllers which provide pulses to the stepper motors for each of the 4 axes of movement.

(f) E34, E35, E36, and E37 – Commercially available PC running under Windows 98 operating system.

(g) E40 – Heating element – Commercially available heater used for temperature control of the target substrate.

(h) E42 – Temperature controller – Provides closed loop temperature control of the print head reservoir.

(i) E43 – Temperature controller – Provides closed loop temperature control of the target substrate mounting plate.

(3) Power supplies

(a) E3 – 5V power supply – An onboard power supply used for miscellaneous machine functions

(b) E4 – 24V power supply - An onboard power supply used for miscellaneous machine functions

(c) E9, E16 – Camera Power Supplies – used to provide power to the CCD cameras used for jet observation and substrate targeting

(4) Printed circuit (PC) boards

(a) E30 – Interconnect module – Facilitates connection between the motion control components (i.e. driving motors and encoders) with the motion control board.

(b) E31 – Motion Control Board – Provides signals to motion control components for desired movements based on programmed positioning from the PC.

(c) E32 – Image processor – Allows feature recognition of fiducials and other identified features based on input from the downward looking CCD camera.

(d) E33 – LAN card – Integral with the system machine control PC, this card allows communication between the system PC and other PCs over a LAN.

(5) Mechanical Systems

(a) Platform systems – This includes the overall machine base, frame, and equipment racks which hold the other subsystems shown in the block diagram.

(i) M1 – Air mover – A motorized blower which will be designed in one of two ways: (a) as a positive pressure blower mounted at the top of the machine to force air down over the printing assembly, or (b) as a negative pressure blower mounted to draw air from the base of the machine.

(ii) M2 – Filter element – HEPA filter elements mounted above the printing assembly to remove air-borne particulates.

(iii) M3 – Air distribution – Duct work incorporated in the machine structure to direct air flow through the machine.

(iv) M4 – Work area light – Overhead fluorescent lighting internal to the machine for operator convenience.

(v) M8 – Camera Mount – An adjustable mounting block for the downward looking camera which rigidly holds the camera in a known location.

(vi) M9 – Camera Mount – An adjustable mounting block for the drop observation camera which rigidly holds the camera in place.

(b) Printing Hardware

(i) M5 – Fluid Reservoir – A stainless steel reservoir equipped for

pneumatic interfaces and a filter for the jetted fluid.
(ii) M6 – Jetting Device – A replaceable unit comprised of a glass capillary surrounded by a PZT element and a rigid metal housing used to generate individual droplets of fluid.

(6) Pneumatic Systems
- (a) P1 – Pressure regulator – Primary pressure control for the machine. Controls pressure supplied by house facilities.
- (b) P2 – Pressure gauge – Analog read-out of machine pressure.
- (c) P3 – Filter – Filter and moisture trap at input to machine pneumatic functions
- (d) P4 – Pressure gauge – Analog read-out of the P5 regulator.
- (e) P5 - Pressure regulator – Provides adjustment of the pressure level supplied to the control regulator.
- (f) P6 – Provides fine adjustment of the pressure level applied to the fluid reservoir.
- (g) P7 – Flow control – Used to provide a controlled flow rate of air to on-board support equipment.

(7) Vacuum Systems
- (a) V1 – Vacuum regulator – Primary control of vacuum level distributed to the machine. Controls vacuum level supplied by house facilities.
- (b) V2 – Vacuum gauge – Analog read-out of machine vacuum level.
- (c) V3 – Vacuum regulator – Provides fine adjustment of the vacuum level provided to the substrate platen.
- (d) V4 – Vacuum gauge – Analog read-out of the substrate platen vacuum level.

(8) Optics Systems
- (a) Downward Looking Optics – Used to location substrate fiducials and inspect deposited drops
  (i) O7 – Video Monitor – Black & White video monitor used to observe the camera output.
  (ii) O8 – CCD Camera – Small profile camera
  (iii) O9 – TV Tube – Image enlargement
  (iv) O10 – Zoom lens to provide various fields of view of the targeted substrate
- (b) Drop Observation camera
  (i) O1 – Video Monitor – Black & White video monitor used to observe the camera output.
  (ii) O2 – CCD Camera – Small profile camera
  (iii) O3 – TV Tube – Image enlargement
  (iv) O4 – Zoom lens to provide various fields of view of the targeted drop formation zone.
  (v) O5 – Fine focus lens – Allows fine adjustment of the image without requiring movement of the camera / lens assembly.

(vi) O6 – Auxiliary lens – Allows greater camera to droplet working distance.

### 5.1.3 Software

The software for the GRIN lens print station will be based on the software used on MicroFab's commercial JetLab™ print stations. The main difference relates to accommodating the rotational axis planned for the GRIN lens print station. We plan to extend the jetLab program to support this type of axis and thereby have the GRIN lens print station benefit directly from future developments for our jetLab™ stations.

A. Overview of Software Structure

(1) Operating system - The GRIN Lens Printing Station program will be based on that currently in use for MicroFab's jetLab™ print stations, with additions to accommodate the rotating chuck feature and to run printing programs directly from CAD file inputs, and it will be designed to run under the Microsoft Windows 98 operating system.

(2) Disk systems - The program will be stored on and run from the hard disk of the control computer. User script files for specific print patterns can reside on other random accessible storage media (floppy disk, ZIP disk, CD). A CD-ROM is usually needed for installation of support software for hardware components (motion control system, image capture and analysis if required), and is de-facto standard equipment on PCs. A high capacity removable (re)writable disk drive is desirable to allow data, graphic and log files generated during the operation of the print station to be copied efficiently to other PCs while keeping the control computer separate from other systems in terms of electronic communications if this is desired. .

(3) User interface - The GRIN Lens Printing Station program will provide a graphical user interface, restricting itself to fairly conventional interface elements (buttons, edit fields, lists, and scroll bars).

### 5.1.3 Bill of Materials

| Qty | U | Description | Mfg. | Mfg's Part No. | MicroFab Part No. | Price Ea. | Price Ext. |
|---|---|---|---|---|---|---|---|
| **1** | **ea** | **Base Machine** | **MicroFab** | | | | **85,570.58** |
| | | | | | | | |
| **1** | | **Substrate Stage** | | | | | **47,420.00** |
| 1 | | 12"x4" X-Y Positioning Stage | Aerotech | ALS20030-M-NC-10-LT30AS-X-Y-CMS | | 16,425.00 | 16,425.00 |
| 1 | | Rotary stage | Aerotech | ADR240-M-59-RE 30X5-M-HM | | 14,745.00 | 14,745.00 |
| 1 | | 4-Axis Motion Controller | Aerotech | U500PCI-ULTRA | | 2,860.00 | 2,860.00 |

| | | | | | | | |
|---|---|---|---|---|---|---|---|
| 1 | | Amplifier chassis | Aerotech | ICM-1900 | | 6,510.00 | 6,510.00 |
| 1 | | Interconnect cable | Aerotech | OP500-12 | | 220.00 | 220.00 |
| 2 | | High accuracy calibration system | Aerotech | HALAR | | 825.00 | 1,650.00 |
| 3 | | Motor feedback cable | Aerotech | BFCD-15 | | 175.00 | 525.00 |
| 2 | | Multiplier box with cable | Aerotech | MX50-D-16M/ & MXC-3 | | 1,085.00 | 2,170.00 |
| 1 | | Right angle L bracket | MicroFab | | | 635.00 | 635.00 |
| 3 | | Motor power cable | Aerotech | BFCD-15 | | 175.00 | 525.00 |
| 1 | | Interface software | Aerotech | COMDISK | | 555.00 | 555.00 |
| 1 | | Vacuum chuck | Galil | DMC1700 Utilities | | **600.00** | 600.00 |
| | | | | | | | |
| **1** | | **Print Head Z-axis Stage** | | | | | **6,835.00** |
| 1 | | 4" stage | Aerotech | ATS150-100-U-40P-NC-BMS-BRK23 | | 6,235.00 | 6,235.00 |
| 1 | | Motor power cable | Aerotech | BFCDMX-15 | | 175.00 | 175.00 |
| 1 | | Motor feedback cable | | | | 175.00 | 175.00 |
| 1 | | Front plate | MicroFab | | | **75.00** | 75.00 |
| 1 | | Back plate | MicroFab | | | **75.00** | 75.00 |
| 2 | | Side plate | MicroFab | | | **50.00** | 100.00 |
| | | | | | | | |
| **1** | | **Motion system integration** | | | | **500.00** | **500.00** |
| | | | | | | | |
| **1** | | **Drive Electronics** | | | | | **6,608.83** |
| 1 | | Waveform generator | Wavetek | Model 395 | | 3,995.00 | 3,995.00 |
| 1 | | Wideband Amplifier | Krohn-Hite | Model 7602M | | 2,400.00 | 2,400.00 |
| 1 | | Strobe Interface Box | MicroFab | | | **100.00** | 100.00 |
| | | Misc. parts | | | | | 113.83 |
| | | | | | | | |
| **1** | | **Pneumatics Panel** | | | | | **1,500.66** |
| 1 | | Enclosure | Allied Electronics | 736-1216 | | 84.60 | 84.60 |
| 1 | | Console Overlay | Adv. Nameplate | | | **82.50** | 82.50 |
| 1 | | Back Panel | | | | **75.00** | 75.00 |
| 1 | | Front Panel | | | | **75.00** | 75.00 |
| 1 | | Console Overlay | Adv. Nameplate | | | **82.50** | 82.50 |
| 1 | | Pressure Gage | C&G Ind. Supply | 2351FCA3 | | 20.00 | 20.00 |
| 1 | | Pressure Regulator | Barton Instru. | 16212 | | 202.30 | 202.30 |

| | | | | | | | |
|---|---|---|---|---|---|---|---|
| 1 | | Vacuum Regulator | McMaster-Carr | | | 44.07 | 44.07 |
| 1 | | Vacuum Gauge | McMaster-Carr | | | 12.07 | 12.07 |
| 2 | | Temperature Controller | Eurotherm | 91E | | 200.00 | 400.00 |
| 1 | | Misc. electrical parts | | | | **300.00** | 422.62 |
| | | | | | | | |
| **1** | | **Vision System** | | | | | **4,648.00** |
| 1 | | CCD Camera | | | | | 670.00 |
| 1 | | Video camera | | STC-400 | | 610.00 | 610.00 |
| 1 | | Power Supply | | 45752 | | 60.00 | 60.00 |
| 1 | | 100C Zoom Module | Optem | 30-11-10 | | 825.00 | 825.00 |
| 1 | | Coax Illum w/ 5mm fine focus | Optem | 30-14-10 | | 475.00 | 475.00 |
| 1 | | Fiber Optic Lamphouse | Optem | 30-16-02 | | 50.00 | 50.00 |
| 1 | | 10mm Fiber Optic Adapter | Optem | 30-16-01 | | 30.00 | 30.00 |
| 1 | | 1X Mini TV tube | Optem | 29-90-90 | | 250.00 | 250.00 |
| 1 | | 2X Auxiliary Lens | Optem | 29-20-41 | | 125.00 | 125.00 |
| 1 | | Light source | | 20500/19 | | 325.00 | 325.00 |
| 1 | | Fiber Optic bundle | | AO8025.40 | | 97.00 | 97.00 |
| 1 | | Video Monitor | Ultrak | KM-12 | | 241.00 | 241.00 |
| 1 | | Image Processing Board | ITI | IC2-COMP-NDOC | | 1,250.00 | 1,250.00 |
| 1 | | Camera adaptor cable | ITI | ACBL-BNC | | 115.00 | 115.00 |
| 1 | | Breakout cable | ITI | BCBL-CAM1 | | 135.00 | 135.00 |
| | | | | | | | |
| **1** | | **Print Head Assemblies** | | | | | **1,100.00** |
| 1 | | Reservoirs | MicroFab | | | **400.00** | 400.00 |
| 2 | | Heaters & Thermocouples | | | | **100.00** | 200.00 |
| 1 | | Jetting Devices | MicroFab | | | **300.00** | 300.00 |
| 1 | | Plumbing/Mounting | | | | **200.00** | 200.00 |
| | | | | | | | |
| **1** | | **Machine Base** | | | | | **11,868.94** |
| ***1*** | | ***Machine Table Base*** | | | | | ***1,686.75*** |
| 1 | | Table | Newport | VH3060W-OPT | | 4,435.00 | 4,435.00 |
| 1 | | Rail | Newport | X95-1 | | **200.00** | 200.00 |
| 1 | | | Newport | CXL95-120 | | **125.00** | 125.00 |
| 2 | | End plate | MicroFab | | | **30.00** | 60.00 |
| 2 | | Supports | MicroFab | | | **80.00** | 160.00 |
| 2 | | HEPA filters | Terra Univer. | 2100-2 | | 169.00 | 338.00 |

| | | | | | | | |
|---|---|---|---|---|---|---|---|
| 6 | | Quad panel latches | Southco | E5-T1-121 | | 3.38 | 20.28 |
| 2 | | Type A Large Mtl. Lift-off | Southco | 96-50-510-50 | | 5.32 | |
| 2 | | Type B Large Mtl. Lift-off | Southco | 96-50-520-50 | | 5.32 | |
| 2 | | Lamp Min Under Cab Light | Home Depot | 662-2-9865 | | 17.82 | |
| 1 | | 5VDC Power Supply | Power One | | | 34.43 | 100.00 |
| 1 | | 24VDC Power Supply | Power One | | | 83.55 | 83.55 |
| 1 | | 50 Pin Flat Cable Interfc | Pheonix | | | 66.60 | 66.60 |
| 4 | | Opto-22 Jumpers | Opto-22 | | | 10.74 | 42.96 |
| 1 | | 20Amp Solid State Relay | Opto-22 | | | 24.78 | 24.78 |
| 1 | | Main Power Switch | Siemens | | | 58.21 | 58.21 |
| 1 | | 20A Circuit Breaker | Siemens | | | 39.15 | 39.15 |
| 12 | | Terminal Block 2.5mm | Siemens | | | 1.35 | 16.20 |
| 10 | | Terminal Block 4mm | Siemens | | | 1.17 | 11.70 |
| 10 | | 10 Pos. Jumper 2.5mm | Siemens | | | 3.67 | 36.70 |
| 1 | | 10 Pos. Jumper 4mm | Siemens | | | 4.57 | 4.57 |
| 6 | | T B Barriers 2.5mm | Siemens | | | 0.60 | 3.60 |
| 2 | | T B End Anchor | Siemens | | | 1.95 | 3.90 |
| 4 | | Y-G Ground Terminal | Siemens | | | 3.90 | 15.60 |
| 2 | | Fuse Block | Siemens | | | 5.70 | 11.40 |
| 2 | | Din Rail | Siemens | | | 10.00 | 20.00 |
| 1 | | Red MTW Wire 18GA | Belden | | | 22.00 | 22.00 |
| 1 | | Blue MTW Wire 18GA | Belden | | | 22.00 | 22.00 |
| 1 | | Green MTW Wire 14GA | Belden | | | 22.00 | 22.00 |
| 1 | | Vacuum Bowl | | | | 25.00 | 25.00 |
| 1 | | Air Regulator & Bowl | | | | 50.00 | 50.00 |
| 1 | | Power Outlet Strip | | | | 10.00 | 10.00 |
| 1 | | Mutiplexer | Opto-22 | | | 97.00 | 97.00 |
| 8 | | Dry Contact Relay | Opto-22 | | | 8.90 | 71.20 |
| 1 | | Input Relay | Opto-22 | | | 8.90 | 8.90 |
| 1 | | Table Mods and Sheet Metal | Regal Res. | | | 5,685.00 | 5,685.00 |
| 1 | | Upper Enclosure | | | | | 1,399.12 |
| 8 | | Stiffener, Door | | | 10531 | 5.48 | 43.84 |
| 4 | | Slide, Door | | | 10533 | 13.05 | 52.20 |
| 4 | | Support, Extrusion | | | 10534 | 19.95 | 79.80 |
| 8 | | Support, Extrusion | | | 10535 | 12.26 | 98.08 |
| 4 | | Support, Extrusion | | | 10536 | 8.96 | 35.84 |
| 4 | | Stiffener, Door | | | 10537 | 5.53 | 22.12 |
| 8 | | Cutting Service | | | | 1.89 | 15.10 |

| | | | | | | | |
|---|---|---|---|---|---|---|---|
| 4 | | Cutting Service | | | | 1.89 | 7.55 |
| 8 | | Square Corner | | | | 17.34 | 138.72 |
| 2 | | Door Slide TOP | | | | 11.20 | 22.40 |
| 2 | | Door Slide BOTT | | | | 11.20 | 22.40 |
| 4 | | Cutting Service | | | | 1.89 | 7.55 |
| 24 | | Joining Plate | | | | 2.65 | 63.60 |
| 48 | | Bolt Kit | | 75-3404 | | 0.43 | 20.54 |
| 8 | | End Fasteners | | 25-3895 | | 1.48 | 11.83 |
| 28 | | Fastners | | 3605 | | 3.01 | 84.25 |
| 4 | | Alum. Panel Hndl. | | 2070 | | 4.28 | 17.14 |
| 4 | | Lexan Door | Ace Acrylics | | 10474 | **50.00** | 200.00 |
| 2 | | Lexan Panel | Ace Acrylics | | 10475 | **125.00** | 250.00 |
| 2 | | Lexan Panel 2 | Ace Acrylics | | 10476 | **125.00** | 250.00 |
| ***1*** | | ***Console Assembly*** | | | | | ***3,098.07*** |
| 1 | | Eurorack, 1800x600x800 Frame | Schroff | 21117-070 | | 570.33 | 570.33 |
| 1 | | 800x600 Side Panels | Schroff | 21117-171 | | 258.3 | 258.30 |
| 1 | | Flush, Solid Top Cover | Schroff | 21117-002 | | 44.97 | 44.97 |
| 4 | | Stationary Shelf | Schroff | 22114-368 | | 55.7 | 222.80 |
| 4 | | Mounting Hardware | Schroff | 22114-349 | | 12.62 | 50.48 |
| 1 | | Cage Nuts M6 | Schroff | 21100-003 | | 9.63 | 9.63 |
| 1 | | Pan Head Screws M6 | Schroff | 21100-021 | | 6.85 | 6.85 |
| 1 | | Washers | Schroff | 21100-015 | | 5.04 | 5.04 |
| 2 | | Bowed side panel | Regal Res. | | 10503 | | 2,500.00 |
| | | | | | | | |
| 1 | | **PC with motion control** | | | | | **2,978.15** |
| 1 | | Personal Computer | Dell | | | **2,129.00** | 2,129.00 |
| 1 | | Optimate 6.5 | Optimus | MIMATE | | 849.15 | 849.15 |
| | | | | | | | |
| **1** | | **Jet Observation Camera** | | | | | **2,111.00** |
| 1 | | CCD Camera | | CV252 | | 670.00 | 670.00 |
| 1 | | Power Supply, 12VDC | | 45752 | | 60.00 | 60.00 |
| 1 | | 2X Rt Angle Obj Tube | Optem | 29-90-96 | | 600.00 | 600.00 |
| 1 | | Zoom 100C Lens | Optem | 30-11-10 | | 825.00 | 825.00 |
| 1 | | 15mm Fine focus module | Optem | 30-13-10 | | 260.00 | 260.00 |
| 1 | | Video Monitor | Ultrak | KM-12 | | 241.00 | 241.00 |
| 1 | | 0.25X Auxiliary Lens | Optem | 29-20-09 | | 125.00 | 125.00 |
| | | | | | | | |

## 5.2 GRIN Lens Modeling: Radial Gradient Case

### 5.2.1 Modeling Concepts

We started our modeling with a generic photographic Wood lens. By photographic we mean the object is placed at infinity in front of the lens. Wood lenses are the lenses of plane-parallel plates with radial gradient. The gradient profile is typically described by the formula as follows:

$$n = N_0 + N_1 \cdot r^2 + N_2 \cdot r^4$$

Here, $N_0$ is the refractive index at the center of the lens, since $N_1$ is less than 0, the refractive index at the edge of the lens is smaller than that at the center. The index difference $\Delta n$ is:

$$\Delta n = N_1 \cdot r^2$$

Initially we set $N_2$ to 0, later we can see that by fine tuning the $N_2$, we can achieve low aberrations without significantly affecting other characteristics (such as focal length) of the lens. In this study, we compared the optical performances of Wood Lens with $\Delta n$ set at 0.1 and 0.2 respectively. Their gradient profiles are shown in **Figure 17**. These values reflect the range of refractive index of the jetable materials currently available to us.

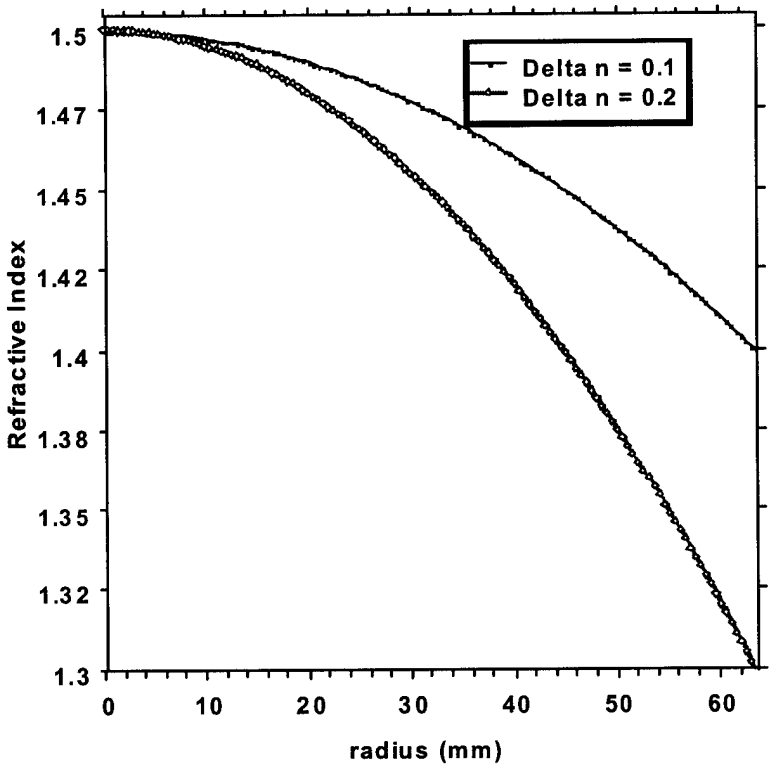


**Figure 17.** *Radial gradient profiles, with Δn of value of 0.1 and 0.2 respectively.*

In **Figures 18-20**, we present the modeling of a 5" (125 mm) Wood lens, showing the change of focal length, RMS spot size and Strehl ratio, respectively, as functions of lens thickness and $\Delta n$. The Strehl ratio is a figure of merit of optical performance which may be defined as the ratio of the total volume under the modulation transfer function (MTF)

of a lens under test to that of a diffraction-limited lens of the same dimensions.[1] We can see that when $\Delta n$ is fixed, the focal length decreases when the thickness of the lens increases. Also we can see the focusing quality (as measured by root-mean-square (RMS) spot size and Strehl ratio) deteriorates as the thickness increases. We also can see when the thickness is fixed, lens with larger $\Delta n$ has shorter focal length and worse focusing quality.

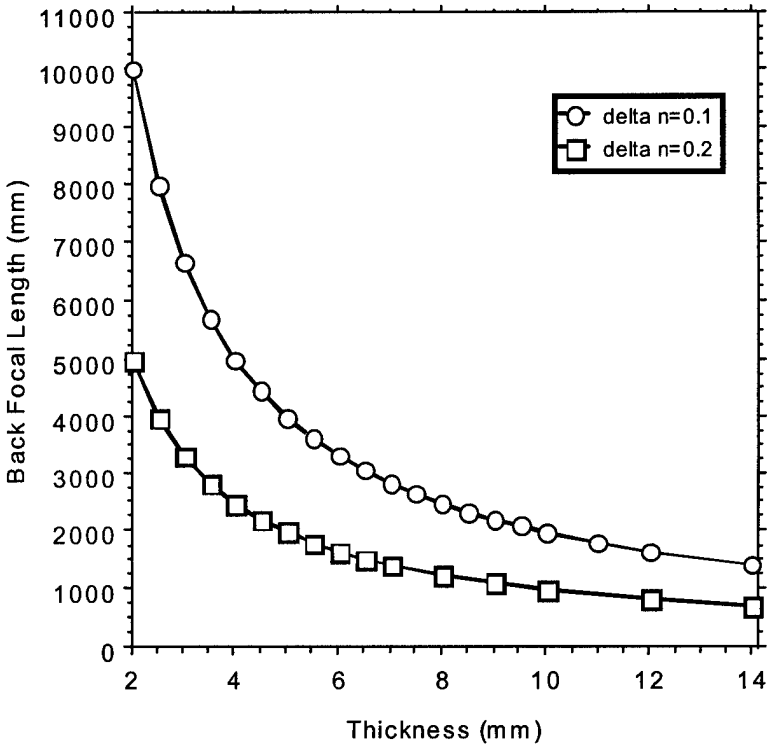


**Figure 18.** *Focal length vs. thickness, with Δn set at 0.1 and 0.2 for a 125 mm diameter Wood lens.*

We also modeled the situations in which $\Delta n$ is fixed and $N_0$ is of different values as shown in **Table 1.** We can see that for a given $\Delta n$, the value of $N_0$ barely affects the performance of the lens. A classical Wood lens design is shown in **Table 2.** We can see that $N_2$ is used for fine tuning of the aberrations. We scale the parameters to the design of 5-inch (125 mm)-diameter Wood lens, which is shown in **Figure 21** together with the performance of the design. Sub-micron RMS spot size and Strehl ratio of 1.0 can be achieved with this design. However, the thickness may be too large for our current printing process. A second design with larger $\Delta n$ is presented in **Figure 22**. It has the same performance (F#, RMS spot size and Strehl ratio), but the thickness is only 1/4 of that of Design I. As we can see, term $N_2$ has great significance

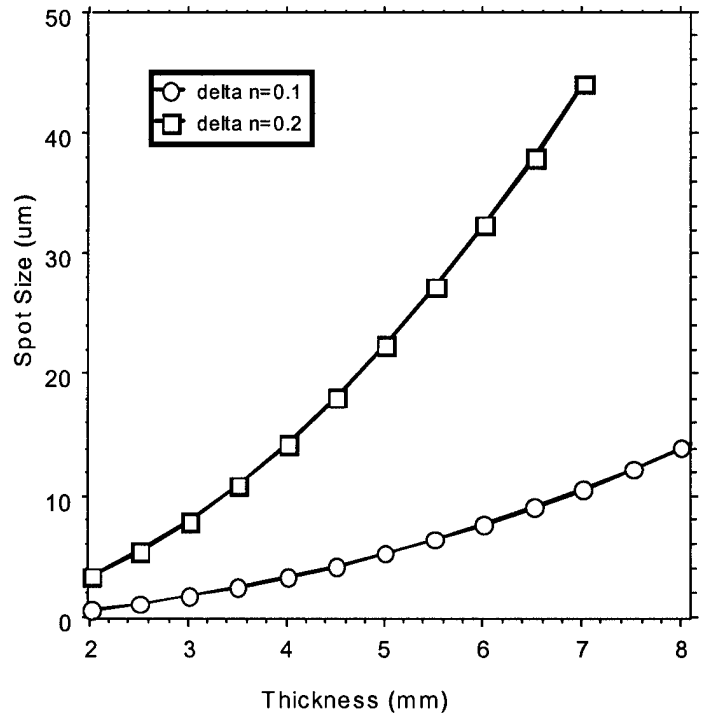


**Figure 19.** *RMS (root mean square) spot size vs. the thickness of the lens of Figure 2 with Δn set at 0.1 and 0.2.*

in these designs. For example, for our second design, if $N_2$ is set to zero, the RMS spot size will be 100 fold larger. Accurately constructing the gradient profile is the key to successfully manufacturing GRIN lens using inkjet process.

**Table 3** summarizes both Design I and Design II.

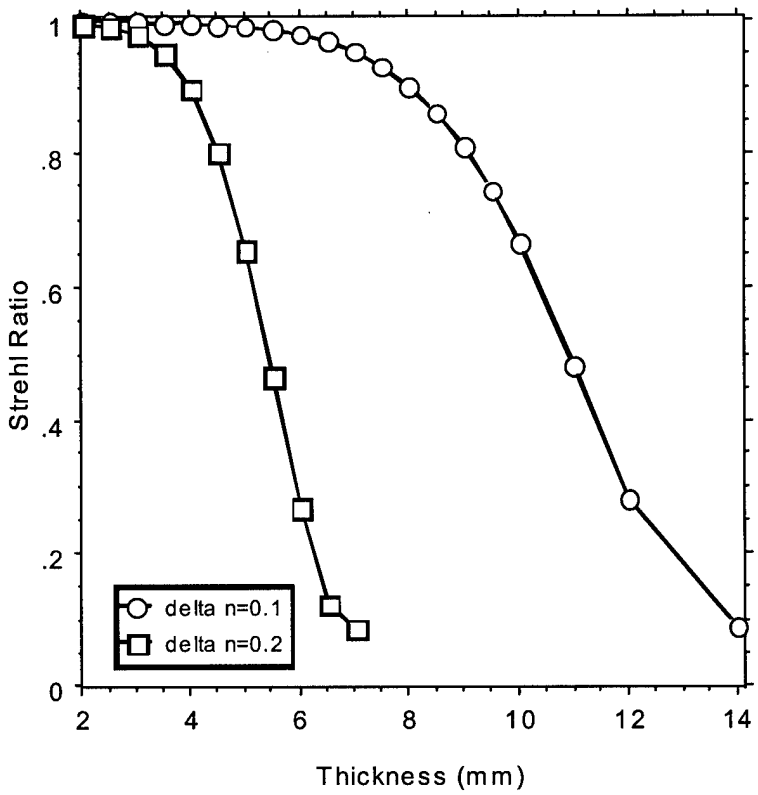


**Figure 20.** *Strehl ratio vs. the thickness of the lens with Δn set at 0.1 and 0.2 respectively.*

**Tabe 1**. *Variation of focal length, RMS spot size and Strehl Ratio as a function of the modeling parameter $N_0$.*

| $N_0$ | Focal Length(mm) | RMS Spot Size (micron) | Strehl Ratio |
|---|---|---|---|
| 1.6 | 3998.94 | 5.17 | 0.995 |
| 1.5 | 3998.87 | 5.34 | 0.994 |
| 1.4 | 3998.79 | 5.54 | 0.994 |

**Table 2**. *Modeling parameters for a classic Wood GRIN lens design.*

| F/No. | F/10 |
|---|---|
| Focal length, **f** | 10 |
| Thickness, **d** | 0.25 |
| $N_0$ | 1.5 |
| C0 | 0 |
| C1 | 0 |
| $N_1$ | -0.20056 |
| $N_2$ | 0.00074 |
| $N_3$ | 0 |

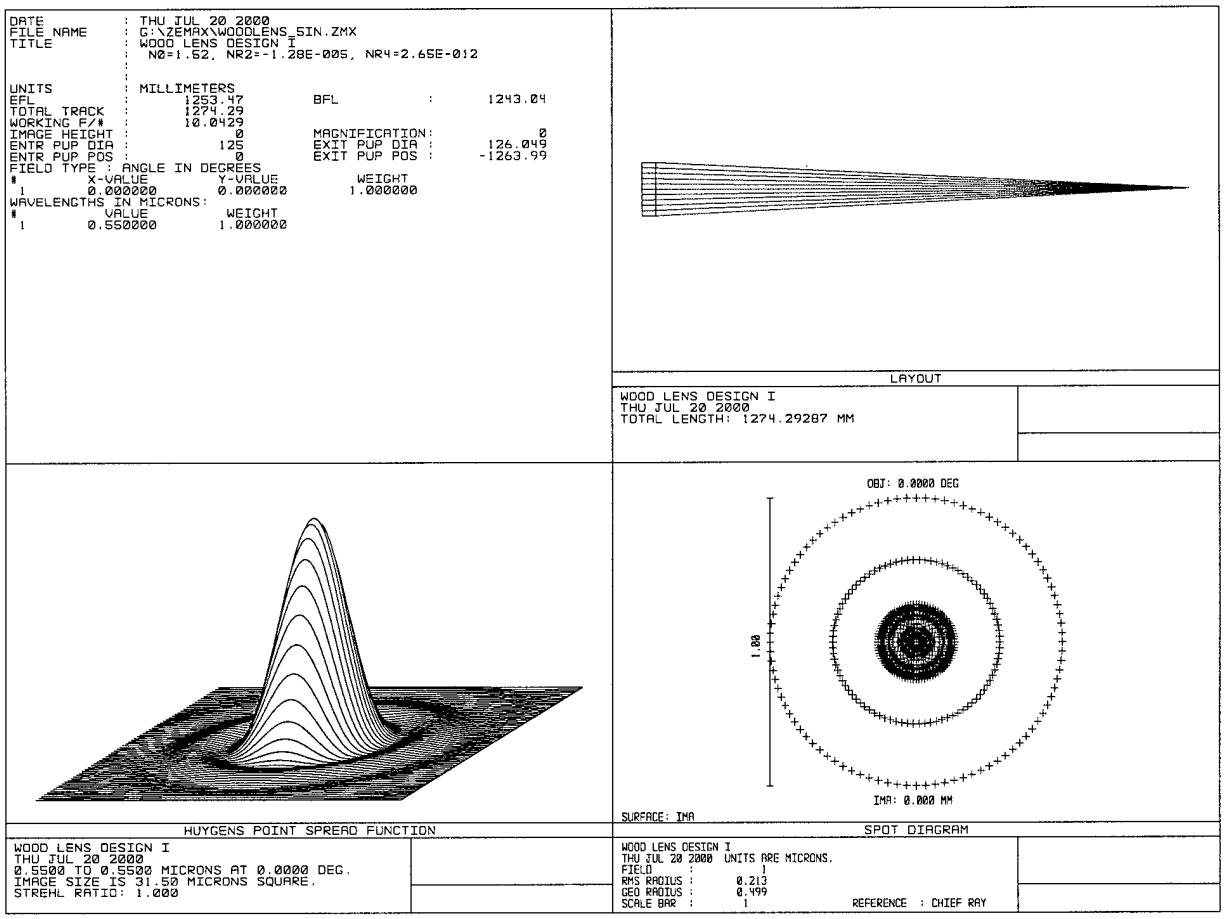


**Figure 21.** *Modeled optical performance of 125 mm diameter Wood lens of Design I of Table 3.*

**Table 3.** *Comparison of two designs of Wood lenses of 125 mm diameter but differing thicknesses.*

| Parameter | Design I | Design II |
|---|---|---|
| F/No. | F/10 | F/10.4 |
| Focal length ***f*** (mm) | 1243.04 | 1331.66 |
| Thickness ***d*** (mm) | 31.25 | 7.5 |
| $N_0$ | 1.52 | 1.52 |
| C0 | 0 | 0 |
| C1 | 0 | 0 |
| $N_1$ | -1.28e-5 | -5e-5 |
| $N_2$ | 2.65e-12 | 9.5e-12 |
| $N_3$ | 0 | 0 |
| Spot Size (um) | 0.27 | 0.56 |
| Strehl Ratio | 1.0 | 0.998 |

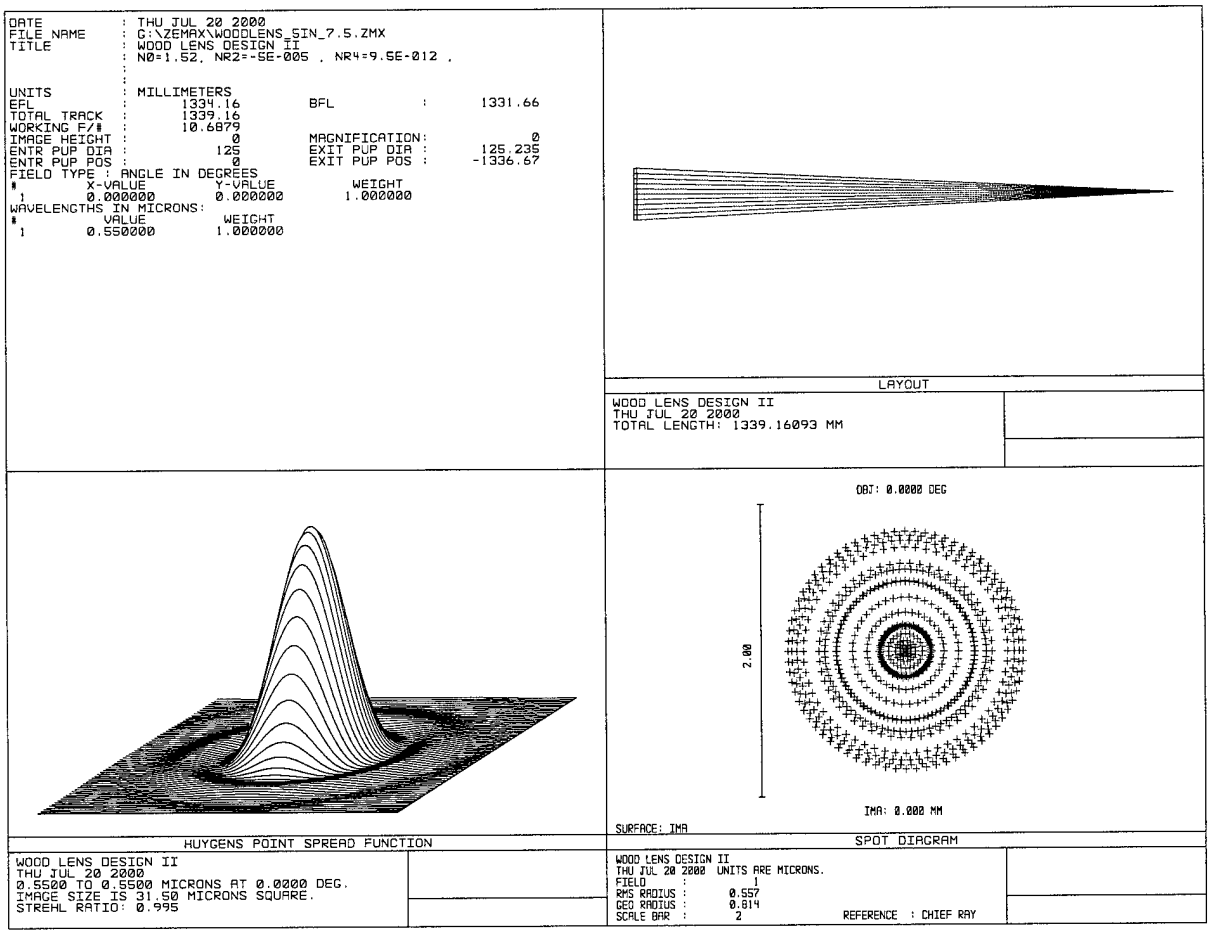


**Figure 22.** *Modeled optical performance ot 125 mm diameter Wood lens Design II of Table 2.*

## 5.2 Lens Performance Optimization

As shown above the optical performance characteristics of a GRIN lens is a result of both its refractive index profile geometry and its physical dimensions. For example, focal length

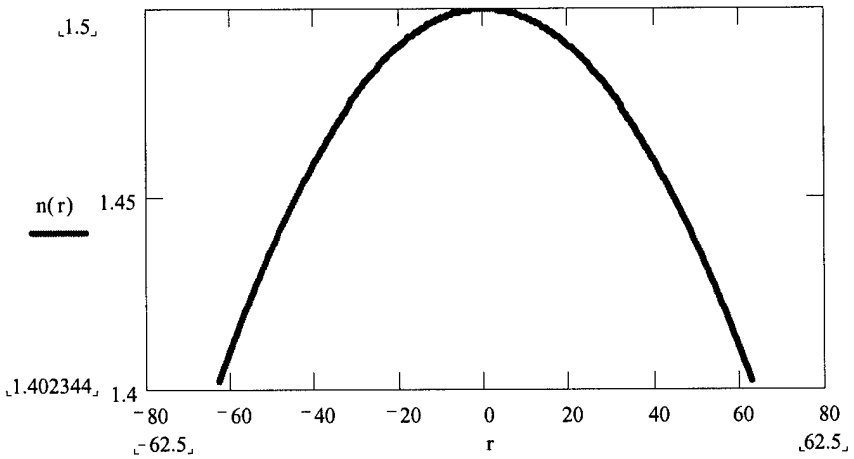


**Figure 23.** *Refractive index profile for a 125 mm diameter radial GRIN lens with index spread from 1.4 to 1.5 (bottom to top of graph).*

and focused spot size achieved with a GRIN lens are both strong functions of the magnitude of the index gradient and the thickness of the lens. This is illustrated in **Figures 23-25** for a 5" diameter AGRIN lens with a parabolic index gradient profile and an index spread of 0.1 (1.4-1.5), where the data was obtained using "ZEMAX - Professional" ray tracing software. In this case it can be seen that optical quality, as judged by minimum focal spot size, decreases while lens focal length decreases exponentially with increasing lens thickness. From the perspectives of an ink-jet-fabrication efficiency and minimization of focal spot sizes, one would want to keep lens thickness to that minimum level required for structural integrity, e.g., 3-5mm for the 125mm lens. On the other hand, if a focal length less than, e.g., 75 cm were required (f/# = focal-length/diameter ≤ 6), the thickness of this lens would need to be at least 30 mm. Thus, the particular application for the lens will always drive the choice of modeled configuration.

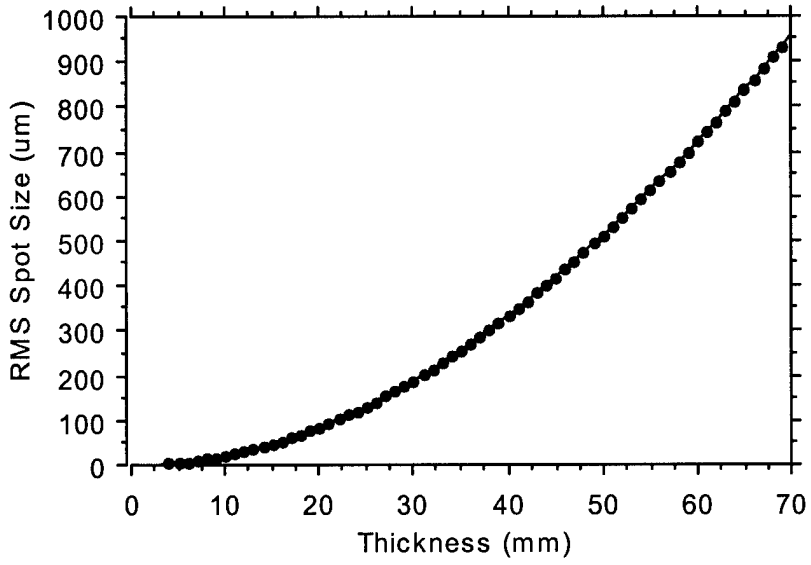


**Figure 24.** *RMS (root mean square) focal spot size versus thickness for GRIN lens of Fig. 23.*

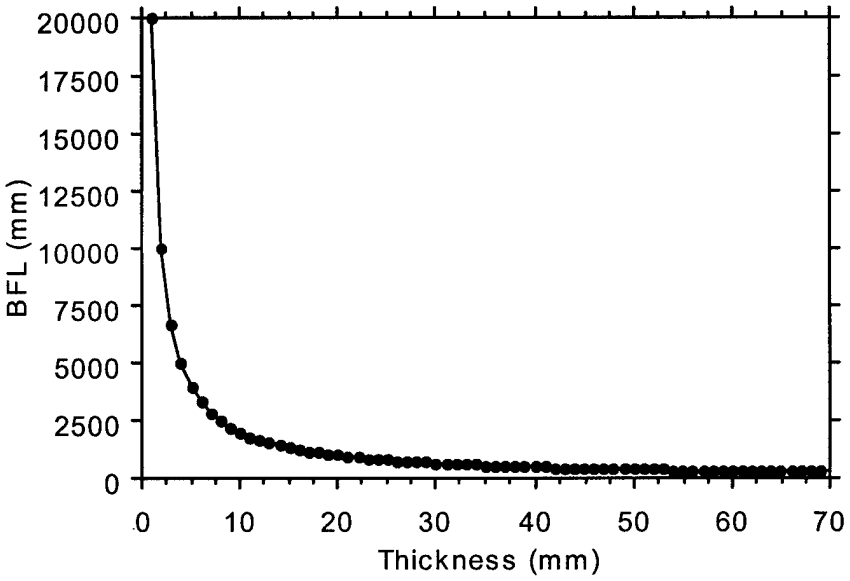


**Figure 25.** *Focal length versus thickness for the GRIN Lens of Fig. 23.*

# References

1. C.S. Williams and O.A. Becklund, *Introduction to the Optical Transfer Function*, John Wiley & Sons, New York, 1989.